

1 **Paleoenvironmental and Geoarchaeological Reconstruction from late Holocene Slope**
2 **Records (Lower Huerva Valley, Ebro Basin, NE Spain)**

3

4 **Pérez-Lambán, Fernando,¹ Peña-Monné, José Luis,² Fanlo-Loras, Javier,¹ Picazo-Millán,**
5 **Jesús V.,¹ Badia-Villas, David,³ Rubio-Fernández, Virginia,⁴ García-Giménez, Rosario,⁵**
6 **Sampietro-Vattuone, María M.⁶**

7

8 ¹Universidad de Zaragoza, Departamento de Ciencias de la Antigüedad, C/ Pedro Cerbuna 12,
9 Zaragoza 50009 (Spain). fperezlamban@gmail.com, javierfanlo@gmail.com,
10 jpicazo@unizar.es

11 ²Universidad de Zaragoza, Departamento de Geografía y Ordenación del Territorio, C/ Pedro
12 Cerbuna 12, Zaragoza 50009 (Spain). jlpena@unizar.es

13 ³Universidad de Zaragoza, Departamento de Ciencias Agrarias y del Medio Natural, Escuela
14 Politécnica Superior, Huesca 22071 (Spain). badia@unizar.es

15 ⁴Universidad Autónoma de Madrid, Departamento de Geografía, Cantoblanco, Madrid, 28049
16 (Spain) virginia.rubio@uam.es

17 ⁵Universidad Autónoma de Madrid, Departamento de Geología y Geoquímica, Cantoblanco,
18 Madrid, 28049 (Spain) rosario.garcia@uam.es

19 ⁶CONICET and Universidad Nacional de Tucumán, Laboratorio de Geoarqueología, San Miguel
20 de Tucumán, 4000, (Argentina) sampietro@tucbbs.com.ar

21

22 **Correspondence author:** Pérez-Lambán, Fernando

23 Universidad de Zaragoza. Facultad de Filosofía y Letras

24 Dpto. Ciencias de la Antigüedad – Prehistoria

25 C/ Pedro Cerbuna 12. 50009, Zaragoza (Spain)

26 Phone: (0034) 654 996 919

27 Email: fperezlamban@gmail.com

28

29

30 **Abstract**

31 Slope deposits, in semiarid regions, are known to be very sensitive environments, especially
32 those that occurred during the minor fluctuations of the late Holocene. In this paper we analyse
33 Holocene colluvium genesis, composition, and paleoenvironmental meaning through the study
34 of slope deposits at Peña Enroque (Ebro Depression, NE Spain). Two cumulative slope stages
35 are described during this period in NE Spain. Both slope accumulations are superimposed and
36 this has enabled an excellent preservation of the aggregative sequence and the paleosols
37 corresponding to stabilisation stages. ¹⁴C and TL dating, as well as archaeological remains,
38 provide considerable chronological precision for this sequence. The origin of the accumulation
39 of the lower unit is placed around 4295-4083 cal yr BP/2346-2134 cal yr BC (late Chalcolithic)
40 and it developed until the Iron Age in a cooler and wetter climate (Cold Iron Age). Under
41 favourable conditions, a soil A-horizon was formed on top of this unit. After a long erosive stage
42 (Warm Roman Period, Medieval Climatic Anomaly), a new slope accumulation was formed
43 during the Little Ice Age. Within the slope two morphogenetic periods are distinguished, both
44 ending with A-horizons. Both periods can be related with the two main cold-wet climatic events
45 in NE Spain.

46

47

48 **Keywords:** Geoarchaeology, slope morpho-dynamic, paleosol, paleoenvironment, late
49 Holocene, Cold Iron Age, Warm Roman Period, Medieval Climatic Anomaly, Little Ice Age, Ebro
50 Depression.

51

52

53

54

55

57 Colluviums are an important source of information regarding the Pleistocene and Holocene
58 sequences and this information can help us understand the paleoenvironmental and genetic
59 processes that have favoured a succession of aggradation and incision stages. There are many
60 studies of slopes with talus flatiron morphologies in semiarid environments in North America
61 and the Mediterranean region (Gerson, 1982; Schmidt, 1988, 1989; Arauzo et al., 1996;
62 Schmidt, 1996; Gutiérrez-Elorza et al., 1998a; Gutiérrez-Elorza et al., 2006; Gutiérrez-Elorza et
63 al., 2010; Boroda et al., 2011). These are generally Pleistocene or early Holocene slopes and
64 so information about Holocene stages is very limited. Also, there are studies in mountainous
65 Mediterranean regions where slopes were generated in cold climatic conditions. But these
66 mountainous colluviums are the result of very specific periglacial and cryonival processes (Van
67 Steijn et al., 1995; Nemeč and Kazanci, 1999; García-Ruiz et al. 2000), which differ greatly to
68 processes that occurred in lower lands.

69 Holocene colluviums are normally poorly preserved but can provide information regarding
70 human activities in the landscape together with paleoclimatic data. The first geomorphological
71 studies of the Holocene colluviums in NE Spain were made by Burillo et al. (1981a, b, 1983) in
72 the Teruel Basin and Albarracín Mountains (Iberian Ranges) at heights of over 1000 masl.
73 These early studies established a close relation between the observed slope stages and
74 Holocene climatic fluctuations, as well as the importance of anthropic factors in some
75 geomorphic processes.

76 Geoarchaeological approaches have since been applied in other areas of NE Spain, at lower
77 altitudes, such as the Ebro Depression (100-400 masl) in the central sector (Peña-Monné et al.,
78 1991), and in the eastern part (Peña-Monné, 1983; Peña-Monné and González-Pérez, 1992;
79 Peña-Monné and Rodanés, 1992; Peña-Monné et al., 1996; Sopena, 1998; Peña-Monné and
80 González-Pérez, 2000; Peña-Monné et al., 2002). There are also some works that synthesise
81 the various stages of the Upper Holocene (Gutiérrez-Elorza and Peña-Monné, 1989, 1992,
82 1998) and offer a general evolutionary model (Peña-Monné et al., 2005) of the
83 geomorphological sequence of aggradation and incision processes in the slopes and infilled
84 valleys of NE Spain, and describe their importance for the study of the geoarchaeological
85 record.

86

87 FIGURE 1

88

89 In this study we analyse the slopes of a rocky spur called Peña Enroque that is located 4 km to
90 the east of the village of Muel and 25 km to the southwest of Zaragoza (Figures 1 and 2). This
91 relief is isolated between open plains formed by Pleistocene pediments and fluvial terraces and
92 secondary valleys filled with sedimentary deposits made during the Holocene (known locally as
93 *vales*). The base level of these geomorphic features is the river Huerva. This geoarchaeological
94 site is representative of the problems that landscape transformations pose to the study of
95 human occupation in the central sector of the Ebro Depression, especially for the Bronze Age
96 and earlier.

97 Holocene colluviums, soils, and archaeological remains are well preserved in Peña Enroque.

98 Because of intense erosion, such a complete assemblage of palaeoenvironmental records is
99 exceptional in drylands. Therefore, their detailed analysis is of great interest for the

100 reconstruction of the evolution of the Holocene and the relationship between climatic

101 fluctuations and human intervention in the landscape. In the Mediterranean region, equivalent

102 case studies are not present in the scientific literature.

103 The main aim of this study is to obtain information about the evolution of the upper Holocene

104 through the description and analysis of sequences of slope stages at Peña Enroque.

105 Aggradation and incision stages have a particular paleoenvironmental meaning that must be

106 considered when studying the Holocene climate and landscape changes, and these can be

107 correlated to global Holocene environmental trends. At the same time, we aim to determine the

108 role that these dynamic environmental fluctuations played in human settlement patterns over

109 the last 4000 years.

110

111

112 **Study area**

113 The lower course of the river Huerva is located in the central sector of the Ebro Depression, in

114 NE Spain (Figure 1). Its upper and middle courses cut through the Iberian Ranges. The general

115 direction of the river flow is south-to-north, joining the river Ebro at the city of Zaragoza. In the

116 Ebro Depression, the river Huerva flows through continental geological formations that were
117 deposited in the Ebro tectonic graben during the Miocene. The main lithologies in the area are
118 lutite, gypsum and limestone – and they maintain their original horizontal arrangement with very
119 few deformations. The resistant upper layers of lacustrine limestone have been modelled into
120 the shape of structural plateaus and mesas (locally called *muelas*), and these are the current
121 outstanding landforms with altitudes over 700 masl (La Muela, La Plana). These high relieves
122 act as the main drainage divides.

123 The current climate of this area is Mediterranean-Continental with semiarid features: annual
124 average mean precipitations are around 400 mm. The rain regime is very irregular and there is
125 an intense hydrological deficit (in the nearby observatory at Zaragoza annual mean precipitation
126 is 345 mm and annual mean evapotranspiration is 1200.7 mm, (Cuadrat et al., 2007)). In fact,
127 this is the most arid inland region of Europe.

128 The landscape is characterised by a Mediterranean-Continental halophile and thermophile
129 steppe (*Rosmarinus officinalis*, *Lygeum spartum*, *Artemisia herba-alba*, *Salsola vermiculata*,
130 *Asphodelus sp.*, *Brachypodium retusum*, *Limonium*) on the slopes and rainfed crop fields on the
131 flat areas (cereals, wines, olives and almonds). This degraded landscape is the result of three
132 main factors: soft lithology, a semiarid climate, and a continuous human occupation since the
133 Mesolithic (Rodanés and Picazo-Millán, 2009) and early Neolithic (Bea-Martínez et al., 2011;
134 Pérez-Lambán et al., 2011). The deforestation rhythm and periods have been determined
135 through the study of Holocene sedimentary infills in the valley bottoms (Peña-Monné et al.,
136 1993; Peña-Monné et al., 1996; Peña-Monné et al., 2001; Peña-Monné et al., 2004; Sancho-
137 Marcén et al., 2008; Constante and Peña-Monné, 2009; Constante et al., 2010; Constante,
138 2011; Constante et al., 2011). Deforestation processes reached significant importance after the
139 Bronze Age and become extremely intense in the Roman Age. The landscape degradation
140 caused by this deforestation has been constant until the present.

141

142

143 **Methods**

144 The methods used in this work are designed to bring together data from different disciplines.

145 Initially, we have drawn in detail an evolutionary geomorphologic cartography of the analyzed

146 area that describes the aggradation and incision stages of the slopes. Several slope profiles
147 were cleared and drawn to scale, with indication of sedimentary units and levels, as well as
148 information regarding sedimentology, stratigraphy, edaphology, palynology, mineralogy,
149 archaeology and chronology. At the same time, a field survey was made to record the
150 archaeological artefact dispersion on the slope and in the profiles. Two of these sections
151 contained archaeological *in situ* remains and were excavated. Finds have been georeferenced
152 in UTM coordinates (ED 50) and drawn on a geomorphologic map (Figure 1).

153 To obtain a better control of the chronology of the geomorphological units, we have sampled
154 charcoal findings in four sections for ¹⁴C dating in laboratories in *Rijksuniversiteit Groningen*
155 (Netherland) and *Universität Zurich-Irchel* (Switzerland). Two pottery shards were also dated by
156 means of TL dating in the Luminescence Laboratory of the *Universidad Autónoma de Madrid*
157 (Spain).

158 Furthermore, the sediments in section 6 were sampled using mineralogical and chemical
159 analysis (Geochemistry Laboratory, *Universidad Autónoma de Madrid*, Spain) and
160 edaphological analysis (*Escuela Politécnica de Huesca*, Spain). More precisely, soil organic
161 carbon (SOC) was determined in the fine soil fraction using the wet oxidation method (Nelson
162 and Sommers, 1982) and organic matter was estimated using the van Bemmelen factor (SOC x
163 1.724). Total carbon was measured using a LECO elemental analyser, and inorganic carbon
164 was estimated by the difference between total and organic carbon and expressed as equivalent
165 calcium carbonate. Electrolytic conductivity (EC) was measured in a 1:1 soil-to-water ratio
166 (Rhoades, 1982). Total phosphorus was calculated by inductively coupled plasma/mass
167 spectrometry (ICP/MS) in a Sciex Elan 6000 Perkin-Elmer spectrometer equipped with an AS91
168 auto-sampler. Palynological analysis was also performed (*Instituto Pirenaico de Ecología*,
169 *C.S.I.C.*, Spain), but unfortunately the results were negative.

170 Finally, we have organised the information provided by the different sampling and analysis
171 strategies and we have correlated the results of Peña Enroque with previous studies on the
172 Holocene environmental changes in NE Spain and with paleoclimate events and
173 paleoenvironmental changes in the Mediterranean and North Atlantic regions.

174
175

176

Results

177 Peña Enroque is a rocky spur (UTM 0655526-4593365; 606 masl) at the extreme of a mesa of
178 Miocene limestone on the western side of the Huerva Valley. It is a long (170 m) and narrow (15
179 to 70 m) landform pointing to the NE (Figure 2). Peña Enroque is formed by a caprock of
180 lacustrine limestone with a 15 m high vertical free face and a talus slope modelled in the lower
181 lutites and marls. This talus gently descends towards the peripheral plains, almost 60 m below
182 the summit. In general terms, the slopes are typically influenced by their orientation in relation to
183 insolation: northern and north-western slopes are more covered by soil and vegetation while
184 south facing slopes are less protected and therefore more eroded. This dissymmetry is due to
185 the differences in water availability and has important consequences for their Holocene
186 evolution.

187

188 FIGURE 2

189

190 In this geomorphic area there are two main zones with archaeological material: the top of the
191 spur and the NW slope (Figure 1). The SE slope also provided some material, but less volume.
192 The summit area is almost flat, and the narrow end is easily isolable because it is surrounded
193 by escarpments around much of its perimeter and the general gradient is 66%. Only the SW
194 flank is accessible. It is, therefore, an ideal defensive position for settlement. There are many
195 similar Bronze Age settlements within a distance of 15 km in the Huerva Valley, such as Los
196 Collados (Jaulín) or San Pablo (Villanueva de Huerva) (Pérez-Lambán et al., 2011).
197 Archaeological remains are sparse because of the rocky bedrock surfaces in most of the
198 summit area. Only the central, slightly depressed area preserves a relict of soil with a few hand-
199 made pottery shards and several ash patches. This depression in the centre of the spur top has
200 been interpreted as the bottom remains of an artificial moat that isolated the original settlement
201 site (Figure 1). The current surface limited by the moat is too little to hold a settlement, but it
202 must be considered that the dimensions of the spur have diminished as a consequence of the
203 retreat of the limestone escarpment. One of the potteries (P3) recovered in the moat was dated
204 by the TL method (Table 1) and its age is 3657 ± 250 yr (MADN-5995BIN). Despite the wide
205 span of the date, it can be chronologically placed in the Bronze Age. As will be later explained,

206 pottery shards similar to the ones found at the spur top have been recovered within the slope
207 accumulations in the NW sector.

208 The other area with archaeological remains is the NW slope. Two significant archaeological
209 contexts were found in this sector: a Bell Beaker pottery accumulation in the basal part of the
210 colluvium (Figure 4, section 4) and a pit excavated in the substratum under the slope (Figure 4,
211 section 5). Both contexts were dated by ¹⁴C analysis of charcoal samples (Table 2). Both dates
212 and potteries belong to the Chalcolithic. In the Huerva Valley, there are other examples of
213 archaeological sites that occupy a slope at the foot of a rocky spur – including the Chalcolithic
214 site known as Peña Roya (Jaulín) (Royo-Guillén et al., 1997).

215

216 TABLE 1

217 TABLE 2

218

219 We can assume that occupation began during the Chalcolithic, at least in the NW sector, and
220 continued during the Bronze Age on the summit of the spur. In addition, it must be added that
221 some medieval and modern pottery shards were also recovered in surface findings, but in such
222 small volumes that permanent occupation is not implied.

223 Two stages of geomorphological slope accumulation were distinguished by means of detailed
224 geomorphological cartography (Figure 1) and field surveys in Peña Enroque. We denominate
225 the older stage lower unit (LwU), which is mainly visible in the NW sector. However, clay
226 quarrying activities have diminished its original extension. In the SE sector, the LwU is also
227 present, but only under the upper unit. The second stage, the upper unit (UpU), is an
228 accumulation that covers most of the remaining slopes. Its gradient is higher and it is affected
229 by the incision of gullies and rills that model the typical talus flatirons landforms. Small alluvial
230 fans are deposited in the surrounding plains at the end of these incisions (Figure 1).

231 The distinction of these two slope colluvium stages is also evident from the study of seven
232 profiles: five of which are in the NW sector (visible in the clay quarry face), and the other two in
233 the SE slope (exhumed by gully incision). These profiles were cleared and cleaned to improve
234 the observation of their stratigraphy. Profiles in sections 1, 6, and 7 best show the existence of
235 the two superimposed stages. In sections 3, 4 and 5 only the LwU is visible, and in section 2 the

236 UpU is shown. The distinction between the two units is mainly erosive, with discordance in the
237 stratification angle. However, in sections 1, 6 and 7 the distinction between the units is
238 characterised by the preservation of a fossilised paleosol with a very apparent buried A-horizon.
239 The internal characteristics of these two stages (LwU and UpU) are best shown in the
240 description of the following sections (Figures 3, 4, 5).

241

242 FIGURE 3

243

244 *Section 1*

245 41°28.665' N, 01°08.226' W; 546 masl. Thickness: 270 cm

246 This profile shows the two aggradation units superimposed one on top of the other (Figure 3,
247 section 1). They can easily be distinguished by their different colour and texture. The LwU lays
248 on the Miocene bedrock that is composed of lutite and marl. The predepositional morphology of
249 the bedrock is irregular. This lower unit is 110-120 cm thick and is composed of very bioturbated
250 dark clay with angular clasts of limestone and dispersed flint (1). Its dark colour is the result of
251 the remobilization and mixing, by means of solifluction processes, of edaphic remains from the
252 upper part of the slope. No edaphological analysis was attempted here because it was not
253 possible to distinguish clear soil horizons. Two hand-made pottery shards (belonging either to
254 the Chalcolithic or the Bronze Age) were found in this unit. The main transportation processes
255 were produced by means of slow solifluction which implies a continuous moisturising of the
256 slope, probably because of snow fusion and in presence of vegetation.

257 The UpU has an erosive base that shows an unclear lineal contact with the LwU. This is
258 because materials from the highest part of the LwU have been remobilized in the base of the
259 UpU (2a). The base is 116-154 cm thick and its ochre colour is very homogeneous. It is formed
260 by angular limestone gravel and some dispersed flint fragments (2b, 2e). The relative
261 homometry of these materials points towards a physical weathering origin (gelifraction,
262 decompression, dry and wet weathering). The main transportation processes observable in the
263 profile are local fluxes, ploughing blocks, some rill channels (2c, 2d), and the textures of washed
264 fine materials. No artificial evidence was found.

265 The processes that formed this unit were very different from those that created the LwU. The
266 UpU formation was a gravity-controlled slope where rock falls from the free face were very
267 active and generated large and small blocks that were transported by gravity and rebound. On a
268 slope with little vegetation, hillside surface water runoff due to occasional but intense rainfalls
269 generated a rill wash of fine materials, while solifluction was of lesser importance. UpU is
270 covered by a thin superficial soil (15 cm) shown in the upper part of the profile.

271

272 *Section 2*

273 41°28.666' N, 01°08.221' W; 542 masl. Thickness: 214 cm

274 Only the UpU (1) is visible in this profile (Figure 3 section 2). It reaches a greater thickness than
275 in section 1 because the LwU lays far below and it is not visible. The unit is composed of
276 several sedimentary layers. The first layer (1a) is a level (90 cm) of angular clasts within a fine
277 ochre-coloured sediment, similar to level 2a of section 1. Rock falls, fluxes and runoff processes
278 prevail at this level. Above it, several levels of homometric gravel and channel structures (1b, 1f)
279 alternate with more clayey levels with disperse clasts (1c, 1d, 1e). The intercalation of flat
280 limestone gravels and a few rounded boulders in level 1d is noteworthy. The whole of the UpU
281 has been formed by sediments being dragged through rills and superficial flow processes, with
282 intense fine sediment wash. All this implies a scarce presence of vegetation on the hillside. This
283 genesis is similar to that of the UpU in section 1. This section contains no archaeological
284 remains.

285

286 *Section 3*

287 41°28.699' N, 01°08.215' W; 518 masl. Thickness: 235 cm

288 This profile is placed in the lower part of the hillside (Figure 3, section 3) in contact with the
289 bottom of the valley. It presents almost only LwU, except for some 10 cm in the upper part of
290 the profile. The basal substrate consists of compact Miocene lutite and marl. Above it, there is a
291 220 cm accumulation of clayey sediment with bioturbation structures, little gastropods, and
292 dispersed charcoals. One of these charcoals in the base of level 1b was dated by means of ¹⁴C
293 to 4581-4413 cal yr BP / 2632-2464 cal yr BC (GrA-47554) (Table 2). There are also some
294 angular limestone clasts and scattered flint fragments. The presence of some stone lines

295 separates different levels, although they are very similar in their characteristics (1a, b, c, d).
296 Above this clayey level there are channels of angular gravels that correspond to the beginning
297 of the upper unit, and which have almost disappeared because of erosion. Finally, on top, there
298 is a surface horizon (15 cm), created by the clay quarrying activities.

299

300 FIGURE 4

301

302 *Section 4*

303 41°28.659' N, 01°08.252' W; 548 masl. Thickness: 47 cm

304 The profile in section 4 is placed in the upper part of the clay quarry (Figure 4). Here the UpU is
305 absent and the LwU is very shallow (20-50 cm). Its composition does not differ from the
306 description of this unit in section 1: dark clays with angular clasts of limestone transported by
307 solifluction processes. In the base there is an erosive channel excavated in the lutite and marl
308 bedrock. Within this channel there was an accumulation of numerous pottery shards
309 corresponding to several vases within an ashen sediment. Some of the pottery shards belong to
310 the Bell Beaker vases (Figure 4) of the late Chalcolithic. ¹⁴C dating of a charcoal resulted in an
311 age of 4295-4083 cal yr BP / 2346-2134 cal yr BC (GrA-45131) (Table 2), which is consequent
312 with the typology of the vases. These archaeological remains were recovered almost *in situ*, as
313 can be deduced by the very limited erosion and dispersion shown by the shards. This fact and
314 their position on the substratum, in the basal part of the accumulation, implies that the age of
315 this archaeological context can be used as *terminus post quem* for the formation of the slope.
316 The potteries from the deposit in section 4 are consistent with surface findings in the NW sector
317 of Peña Enroque. There are clear diagnosis features that coincide with the ¹⁴C dating. Some
318 morpho-technological elements of the potteries are related to the end of the Chalcolithic and the
319 beginning of the Bronze Age: such as the basal basket impressions (Rovira i Port, 2006);
320 peripheral impressions in the outstanding edges of the mouth of the vessels – as is also found
321 at the site of Peña Roya (Royo-Guillén et al., 1997); or the accentuated shoulders as in the
322 case of vessels recovered at Los Collados. In addition to these clarifying features, the presence
323 of several Bell Beaker fragments confirms the chronological dating of the deposit to the late
324 Chalcolithic.

325

326 *Section 5*

327 41°28.675' N, 01°08.303' W; 537 masl. Thickness: 336 cm.

328 This is the thickest section. It is placed in the lower part of the hillside, in contact with the valley
329 bottom. In its profile (Figure 4, section 5), in addition to the LwU and UpU, there is a previous
330 unit (Pre-LwU).

331 This first unit is formed of three deposits. The first (0a) was deposited on a small stream bed on
332 the substratum of clay and marls. It is formed of small gravel and clay. However, it is only
333 partially visible because it was cut and removed by the artificial excavation of a pit that holds the
334 second deposit (0b). The vertical section of this structure has the shape of a truncated cone,
335 and its horizontal section is oval. The pit was filled with alternated levels of clayey sediment and
336 ashes rich in charcoal. The only archaeological remains recovered in this unit were three flint
337 flakes or chunks. ¹⁴C dating of a charcoal sample from the ash levels resulted in 5295-5037 cal
338 yr BP / 3346-3088 cal yr BC (GrA-50207) (Table 2). This second unit seems to have also been
339 cut by a shallow pit or depression that forms the third deposit (0c). This deposit is formed of
340 homometric angular clay fragments (5-10 cm), something that is incompatible with the natural
341 fragmentation, transport, and deposition that would cause erosion and a disaggregation of the
342 blocks. This deposit therefore seems to have an anthropic origin.

343 The LwU (1) lays above the Pre-LwU unit. There are several intercalated sub-horizontal levels
344 inside. Some of these levels share their features with those described in other sections.

345 However, others have different materials and structures. Thus, level 1b holds a series of large-
346 medium flat angular clasts in a horizontal disposition. Level 1e has a typical channel structure
347 filled with gravel and clay. In addition to this, there are dark layers (1f) that may be related to
348 stages of stabilisation, and therefore with accumulation of organic material resembling an A-
349 horizon paleosol. The UpU lays on the paleosol. In the base of this unit there is a horizontal
350 layer of clasts (2a). Above these clasts, level 2b has been affected by agricultural activities.

351

352 FIGURE 5

353

354 *Section 6*

355 41°28.517' N, 01°08.192' W; 536 masl. Thickness: 250 cm

356 This is one of two sections located in the gully incisions on the SE hillside (Figure 1). The basal
357 part of the visible profile is formed of 1 m of the LwU. However, the incision does not reach the
358 Miocene substratum and so the real thickness of this unit remains unknown. At this point, the
359 LwU is formed of abundant clay and some small gravel (1a). Above the LwU, a 0.25-0.30 m
360 thick A-horizon paleosol has developed (1b, horizon IIIA), perfectly distinguishable because its
361 colour is darker than any other level (Figure 5, section 6).

362 Above this paleosol there is a 1 m accumulation of limestone clasts and large blocks in a clayed
363 matrix corresponding to the upper unit. The contact between it and the upper surface of the
364 paleosol is irregular. The UpU is well stratified and the gradient of its levels is higher than that
365 observed in the LwU. In the higher part of the section, there can be observed two slightly darker
366 layers that are equally interpreted as A-horizons from paleosols (2b and 2d, horizons IIA and
367 IA_h, respectively). The upper part is cut by the current slope topography (Figure 6).

368 No archaeological remains or charcoal samples were recovered in this section. Some charred
369 small roots were found, but these were unsuitable for ¹⁴C because their origin was uncertain.

370

371 FIGURE 6

372

373 Analysis of paleosols from section 6

374 In this and the following section, the existence of a preserved continuous paleosol is of great
375 relevance. For this reason, it has been analysed using palynological and edaphological
376 methods. Palynological analysis gave negative results because the pollen was too poorly
377 preserved and the pollen count was not statistically representative. Physical and chemical
378 properties of the soil (Table 3) were much more informative.

379

380 TABLE 3

381

382 In the soil that was sampled (Section 6), successive discontinuities were observed through the
383 presence of stone lines and the heterogeneous distribution of particles, in both gravel (>2 mm of
384 diameter) and fine earth (< 2 mm) fractions. The rock fragments are Miocene limestones, mainly

385 fine and medium gravel (2-60 mm; occasional boulders of 200-600 mm in IIC2), angular
386 shaped, and fresh or slightly weathered; the content being higher in the first two profile metres.
387 For all horizons, the particle size distribution is fine, with a predominance of clay and silt
388 fractions.
389 In addition to the sub-current IAh horizon (profile level 2d), two buried horizons (IIA, profile level
390 2b, 90 to 110 cm deep, and IIIA, profile level 1b, 170 to 200 cm deep) were found. These A-
391 horizons have an organic matter content of about 4%, a C/N ratio of between 18-30, and
392 phosphorus content from 200 to 280 mg/kg – in all cases higher values than the underlying B or
393 C-horizons. Moreover, A-horizons have a lower Munsell value (inversely related to soil organic
394 matter); as well as lower soluble salt (EC) and calcium carbonate contents than their respective
395 underlying horizons. These chemical and physical properties show that the soil (and therefore,
396 the aggradation process) had two periods of stability, when more soluble salts were washed
397 away and fresh organic matter and some major nutrients such as phosphorus were
398 accumulated on the A-horizon surfaces.

399 The sub-current paleosol (IAh-IC) and the intermediate paleosol (IIA-IIC) are classified as *Haplic*
400 *Regosol (calcaric, skeletal)* for IUSS (2007). The third buried paleosol is also an *Haplic Regosol*,
401 but shows a slightly larger development (IIIA-IIIBw-IIIC), which could have evolved to *Haplic*
402 *Calcisol*, according to the soil chronosequences studied in these semiarid environments (Badía-
403 Villas et al., 2009). There are very weakly developed mineral soils that are deep, well drained,
404 and derived from unconsolidated materials. Regosols correlate with *sols peu évolués*
405 *régosoliques d'érosion* (Baize and Girard, 2009) or Entisols (Soil Taxonomy Staff, 2010).

406

407 *Section 7*

408 41°28.534' N, 01°08.193' W; 531 masl. Thickness: 238 cm

409 This section is similar to the previous section. Some 130 cm of LwU is seen (Figure 5). The
410 upper part of this unit (1d) is formed of a 25-35 cm thick dark layer (level 1d in section 7) that
411 corresponds to IIIA-horizon in section 6 and is present in all incisions in the SE sector of Peña
412 Enroque. Inside this A-horizon there is a small groove (45 cm wide and 12 cm deep) that
413 contains a considerable amount of organic material, ashes from a hearth, and a few charcoal
414 fragments. ¹⁴C dating of one of these fragments gave the date of 2152-1995 cal yr BP / 203-46

415 cal yr BC (UZ-5952 / ETH-42556) (Table 2). The upper part of this hearth is covered by a
416 limestone slab severely altered by fire. This paleosol equals that described in section 6,
417 although in this case it can be termed *Technic Calcisol* because of its important anthropic
418 traces.
419 On top of the paleosol, the UpU (2) is 75 cm thick and its characteristics are very similar to
420 those described in section 6. In the upper part of this section three pottery shards were
421 recovered. Their typology belongs to the 17th to 19th centuries. One of them was also dated by
422 means of TL to 387 ± 21 yr (MADN-5998BIN) (Table 1), that is, 17th century.

423

424

425 **Discussion**

426 From the information obtained through the study of the seven sections we can establish the
427 series of evolutionary stages at Peña Enroque (Figure 7). This sequence can be related to the
428 different Holocene climate periods and human occupation phases.

429

430 **FIGURE 7**

431

432 *The pre-lower unit (Pre-LwU)*

433 As stated previously, sections 1 and 4 show a very irregular erosive contact between the
434 substratum and the LwU. This is evidence of the existence of an actively erosive stage previous
435 to the LwU (Pre-LwU). During this stage, the landscape would have been characterised by the
436 presence of widespread gullies and rills, producing extensive badlands on the Miocene clay and
437 marls. Section 5 shows the artificial excavation of a pit in a thin accumulative level (Figure 4,
438 section 5, level 0a) with clayey substratum, that is in a mainly erosive area (Figures 7, 1; and 8).
439 The date (Pre-LwU) can be chronologically placed thanks to the existing ¹⁴C dating (5295-5037
440 cal yr BP / 3346-3088 cal yr BC, GrA-50207) from the artificial pit. This date falls between two
441 chrono-cultural periods: the end of the Neolithic (5500-2700 BC) and the beginning of the
442 Chalcolithic (2700-2100 BC). Moreover, this Pre-LwU must be previous to the important
443 accumulations of the LwU, whose base dates are between 4581-4413 cal yr BP / 2632-2464 cal

444 yr BC (GrA-47554) (section 3) and 4295-4083 cal yr BP / 2346-2134 cal yr BC (GrA-45131)
445 (section 4) or the late Chalcolithic.

446 From the paleoenvironmental point of view, Jalut et al. (2000) indicate that the Mediterranean
447 region was experiencing a dry stage in the Pre-LwU phase, coherently with the aridity
448 generated in Southern Europe and the Near East during the 4.2 event (Bond et al., 1997). The
449 RCC (rapid climate change) established by Mayewski et al. (2004) for 4200-3800 BP would also
450 coincide with this dry environment stage (Figure 9). We can deduce a climate with scarce but
451 concentrated precipitations (similar to the current pattern) that would prevent the accumulation
452 and stabilisation of slopes and would favour the incision of gullies and rills. This erosive stage
453 must have been widespread across NE Spain, since slopes of this or previous periods have
454 never been found. The only exceptions are some rarely preserved much older slope formations
455 from the Pleistocene and early Holocene (Arauzo et al., 1996; Gutiérrez-Elorza et al., 1998a;
456 Gutiérrez-Elorza et al., 2006; Gutiérrez-Elorza et al., 2010). At the same time, since the
457 Neolithic (5500-2700 BC) the tributary valleys in the region underwent an aggradation process
458 that evidences an increase in erosion in the slopes of the tributary basins of the river Huerva,
459 and reaching high erosion rates before the Bronze Age (Peña-Monné et al., 1993; Peña-Monné
460 et al., 2001; Peña-Monné et al., 2004; Peña-Monné et al., 2005; Constante et al., 2010;
461 Constante, 2011; Constante et al., 2011).

462 In NE Spain there are no other descriptions of evidence of this Pre-LwU erosive stage.
463 However, its existence was suggested in Burillo et al. (1981a, b) and Gutiérrez-Elorza and
464 Peña-Monné (1998) as a result of the observation of erosive morphologies previous to the LwU,
465 and termed the *Post-Bronze Age Slope*. This erosive stage was also taken into account in the
466 Ebro Depression Holocene evolution model established by Peña-Monné et al. (2005).

467

468 FIGURE 8

469 FIGURE 9

470

471 *The lower unit (LwU)*

472 The study of the slopes of Peña Enroque revealed an abrupt change from the late Chalcolithic.
473 The new prevailing process is a large aggradation dynamic in the slopes that is visible both in
474 the cartography (Figure 1) and in the profiles of the sections (Figures. 3, 4, and 5).
475 The LwU accumulated on a paleorelief of irregular morphology and generated a complete
476 superficial regularisation by means of a long lasting accumulative process. Pottery shards in the
477 base of this unit (section 4) and the ¹⁴C datings of the lower levels in sections 3 and 4 indicate
478 the initial moment of the sedimentation of the slope (Figure 8). It is interesting to highlight that in
479 section 4, the dates belong to pottery and charcoal which were found *in situ* or just slightly
480 displaced. This circumstance gives great precision to the identification of the beginning of the
481 aggradation (4295-4083 cal yr BP / 2346-2134 cal yr BC, GrA-45131). However, the dating in
482 4581-4413 cal yr BP / 2632-2464 cal yr BC (GrA-47554) in the base of section 3 must be
483 considered the least precise *post-quem* date, as it was performed on a charcoal that was much
484 displaced as a result of the slope processes. Therefore, the beginning of this regularising stage
485 must be approximately placed in the late Chalcolithic, around 4295-4083 cal yr BP / 2346-2134
486 cal yr BC (GrA-45131). This meant that for the first time the starting point of the LwU had been
487 determined with precision. This late Chalcolithic origin of the LwU was first considered after the
488 finding of a Chalcolithic arrow tip and the 4654-4384 cal yr BP / 2705-2435 cal yr BC ¹⁴C dating
489 of a charcoal (Picazo-Millán and Perales-García, 1994; Picazo-Millán, 1999-2000) from within a
490 slope at the Alfambra Castle in the Iberian Range (Teruel, Spain). However, unlike the dating in
491 Peña Enroque, the chronology from Alfambra was not obtained from *in situ* findings, and so the
492 beginning of the accumulation was not so well determined.

493 In addition to this, in the intermediate levels of section 1 some hand-made pottery shards were
494 found. However their chrono-typology is less clear and they may belong either to late
495 Chalcolithic or to a broad part of the Bronze Age, that is, between 2500 and 1500 BC. As they
496 are not *in situ* findings, their dating value is *post-quem*, indicating that the slope formation
497 continues after their chronology. These shards must have been transported from the upper area
498 of the slope or even from the summit of Peña Enroque, where, as already indicated, a
499 settlement with a defensive moat was located.

500 Except for the abovementioned pottery, in Peña Enroque we lack dating evidence for the upper
501 levels of the LwU. However, in other slopes in NE Spain, the development of this accumulation

502 stage has been observed during the early, middle, and late Bronze Age (Burillo et al., 1981a, b,
503 1983; Peña-Monné and González-Pérez, 1992; Peña-Monné et al., 1996; Peña-Monné and
504 González-Pérez, 2000; Peña-Monné et al., 2002) and even during the Iron Age (Picazo-Millán
505 and Perales-García, 1994). The accumulation stage never reaches the Iberian Period (>500
506 BC), as the archaeological remains of that and later periods are located above these slopes and
507 act as *terminus ante-quem* for the accumulation (Peña-Monné et al., 2005). Some works on
508 slope stages and talus flatiron formations in nearby areas in the Ebro Depression (Arauzo et al.,
509 1996; Gutiérrez-Elorza et al., 1998a; Gutiérrez-Elorza et al., 1998b; Gutiérrez-Elorza et al.,
510 2006; Gutiérrez-Elorza et al., 2010) provide further charcoal ¹⁴C dating (2930 ± 60 BP, 2529 ±
511 52 BP; 2480 ± 80 BP) for Holocene regularisations, and some contain Bronze Age pottery.
512 Therefore, we can conclude that the formation of the LwU spans from the 4295-4083 cal yr BP /
513 2346-2134 cal yr BC (GrA-45131) to the 700-550 BC, resulting in a generalised morphological
514 regularisation of the established slopes (Figure 7, 2). Their concave profile would have begun in
515 the higher part of the upper escarpment of the hill or platform, as is seen in the NW slope of
516 Peña Enroque, and extend to the basal concavity connected to the nearby valley bottoms.
517 An important aspect of the evolution of the LwU is the development of an A-horizon, clearly
518 visible in sections 1, 5, 6 and 7, and preserved thanks to the superposition of the later UpU. The
519 date obtained from an *in situ* charcoal of a hearth inside the A-horizon from the paleosol in
520 section 7 is 2152-1995 cal yr BP / 203-46 cal yr BC (UZ-5952 / ETH-42556). This signifies that
521 its edaphic development reaches at least the Ibero-Roman Period.
522 The characteristics of the paleosol in section 6, especially its 1b level (horizon IIIA, Table 3),
523 make it clear that it was formed in a stable stage which was long enough to allow the formation
524 of a B-horizon and achieve a low salt content and a high concentration of organic material and
525 phosphorus. From a physical and chemical point of view, the IIIA horizon has the highest
526 productivity potential of all the analysed edaphic horizons in the profile in section 6. Its organic
527 matter, nitrogen, and phosphorous values are higher than the values of the other two A-
528 horizons (IIA and IA_h). Its granulometric composition and well structured thick horizons (B_w)
529 favour a greater water reservoir capacity and it contains evidence of intense biological activity.
530 These hydrologic and biotic characteristics of the IIIA horizon reinforce its interest as a
531 potentially productive soil. However, no evidence of anthropic use was found in this paleosol.

532 The most frequently used chemical indicators of anthropic intervention on the soils are N, K, P,
533 Ca, Mg, organic matter and pH (Leonardi et al., 1999; Branch et al., 2007). Of these, Ca and Mg
534 are not very significant in dry limestone environments, and there is little doubt that the most
535 important is phosphorous (Eidt, 1977; Schlezinger and Howes, 2000). P levels in horizon IIIA in
536 the profile in section 6, as well as the other indicated parameters, are lower than what is
537 normally registered in human used paleosols in semiarid environments (Roldán et al., 2008;
538 Sampietro et al., 2011). Therefore we must assume that the surface of this paleosol in Peña
539 Enroque was never used for anthropic activities. This circumstance can explain why it was so
540 well preserved and active (as it was protected by undisturbed vegetation) until Roman times. In
541 addition to the lack of evidence of anthropic use of the paleosol in the analysed profile, the fact
542 of its existence is of great importance as it demonstrates the presence of productive soils for
543 agriculture and cattle in this region until the Roman times. Erosion has reduced the extension of
544 favourable pedological components, and these have almost disappeared from the current
545 landscape.

546 The study of the sections and geomorphologic characteristics of the LwU provide enough
547 features for its paleoenvironmental characterisation. The prevalence of solifluction processes,
548 with an abundance of clay, can be related to humid conditions, as was stated by Gutiérrez-
549 Elorza and Peña-Monné (1998), who argued that the slopes of this stage are the result of a
550 regime of precipitations that were not very intense – so preventing drain concentration while
551 favouring water infiltration. Paleoenvironmental reconstructions of the Upper Holocene comprise
552 cold and humid conditions for the Bronze and Iron Ages on a global scale (Lamb, 1977) and in
553 the Mediterranean region (Bintliff, 1982). This moment coincides with Iron Cold Age (Gribbin
554 and Lamb, 1978), in the transition between the Subboreal and the Subatlantic. Lamb (1977)
555 calculates annual mean temperatures around 2° C below present day values. This could be
556 enough to favour higher rates of winter snowfall and, therefore, the presence of melt water that
557 moisturises the slopes. The relationship of these slopes with a climate which was cooler than
558 today was already determined in the very first geoarchaeological studies of Holocene slopes
559 (Burillo et al., 1981a, b, 1983). This relation has also been used to explain Pleistocene slope
560 accumulations in the N and NE of Spain (Sancho-Marcén et al., 1988; Arauzo et al., 1996;

561 Gutiérrez-Elorza et al., 1998a; Gutiérrez-Elorza et al., 1998b; Gutiérrez-Elorza et al., 2006;
562 Gutiérrez-Elorza et al., 2010) that share similarities with respect to their genetic processes.
563 For the Upper Holocene this stage matches with the 2.8 event of Bond et al. (1997) or the 2.6
564 event of Van Geel et al. (1996), who place the climax of this cooling stage around 800-600 BC.
565 Moreover, the RCC (rapid climate change) pointed out by Mayewski et al. (2004) between 3500
566 and 2500 BP on the basis of GISP2 and other indicators covers the chronology of the formation
567 of the LwU slopes in the Huerva Valley (Figure 9). Additionally, the existence of humid
568 conditions for this chronological period in a closer area can be observed in the data regarding
569 paleofloods in Spain provided by Thorndycraft and Benito (2006) and Benito et al. (2008), or in
570 the high lake levels in the central sector of the Ebro Basin (Gutiérrez-Elorza et al., 2012 (in
571 press)) and the Pyrenees (Corella et al., 2011a; Corella et al., 2011b). Moreover, the
572 aggradation in the Holocene infills of the valleys near Peña Enroque evidences an environment
573 that was wetter than today (Peña-Monné et al., 2004; Sancho-Marcén et al., 2008; Constante et
574 al., 2009; Constante et al., 2010; Constante et al., 2011).

575

576 *Erosive stage between LwU and UpU (Inter LwU-UpU)*

577 Slopes of the LwU were partially removed by an erosive stage after the Bronze and Iron Ages,
578 but before the formation of the UpU, also called *Post-Medieval regularisation* (Figure 7, 3).
579 Possibly, before the removal of the slope, talus flatirons morphologies would have been formed
580 as intermediate gullies separating triangular slope facets. This can be observed in other reliefs
581 in the Ebro Depression.
582 In previous studies concerning this sector of the Huerva and the Ebro valleys, the beginning of
583 this erosive stage was placed in the Ibero-Roman period. This stage generated important
584 accumulative infills in the nearby valley bottoms (Peña-Monné et al., 2004; Peña-Monné et al.,
585 2005; Constante et al., 2010; Constante, 2011; Constante et al., 2011). The characteristic
586 dynamics inferred from the sediments in these valleys match with climate conditions similar to
587 the present day: short, intense, and frequently stormy precipitations that favoured the formation
588 of gullies. In addition to the climatic cause, it is necessary to consider the action of a major
589 human intervention in the landscape that is characteristic in this region following the Iberian
590 period and especially during the Imperial Roman times (as registered in the valley infills). These

591 sediments have a prevalence of fine grain materials that come from the washing of the soils of
592 the slopes and they contain continuous charcoal levels as a result of generalised deforestation
593 (Peña-Monné et al., 1993; Peña-Monné et al., 2001; Peña-Monné et al., 2004). Consequently,
594 in the erosive processes of this stage, the lack of vegetation cover due to anthropic
595 deforestation has played an important role.

596 This erosion also led to the re-activation of the escarpment retreat processes by means of basal
597 sapping, lateral decompression of limestone free faces, and rock falls. This would have affected
598 the settlements placed on the hilltops and platforms, as they would lose much of their surface
599 and perimeter. Given the great quantity of material that fed the slopes during their several
600 formational stages and from the escarpment retreat rate – which is quantified at 0.9-1 m/ka in
601 this semiarid region (Arauzo et al., 1996; Gutiérrez-Elorza et al., 1998a; Gutiérrez-Elorza et al.,
602 1998b; Peña-Monné et al., 2005; Constante, 2011) – it can be inferred that the summit in Peña
603 Enroque was much larger and due to the easily erodible lithological components, possibly even
604 double the current surface.

605 Chronologically, this erosive stage must be placed after the LwU and before the new slope
606 generated during the LIA, that is, in a chronological range that includes the Ibero-Roman period
607 and the Middle Ages, without the possibility of further precision, at least for the moment (Figure
608 9). Environmental conditions related to this stage are found in the Warm Roman and Medieval
609 Periods and completely described in paleoclimatic literature (Maasch et al., 2005). Jalut et al.
610 (2000) point out two phases of increased aridity in the Western Mediterranean during this
611 temporal *lapsus*. Moreno et al. (2012) gather information about the influence of the Warm
612 Medieval Period – the Medieval Climate Anomaly – in the evolution of the palynological lake
613 and marine records in the Iberian Peninsula. These records show a prevalence of xerophytic
614 and heliophytic taxas between AD 900 and 1300 in the Mediterranean area – in contrast with
615 the more humid north of Spain. Similarly, in Roberts et al. (2008; 2012) there is contrasting
616 palaeolimnological data concerning the humidity of the western (drier) and the eastern
617 Mediterranean (wetter). Finally, this stage is placed between the RCC 4 and 6 events of
618 Mayewski et al. (2004), with a cooler interruption in RCC 5 (1200-1000 BP).

619 As a consequence of this erosive stage, the LwU has disappeared almost completely in many
620 areas of the Ebro Depression. The preservation of the LwU is conditioned by the orientations of

621 the slope. Southern slopes are severely eroded, while northern slopes preserve part of the LwU
622 regularisation. Numerous archaeological sites were altered by the formation of the LwU and
623 were further degraded during this erosive stage, resulting in a significant loss of information
624 about human occupation in late Prehistory. This can explain the almost complete absence of
625 remains for these periods in this region.

626

627 *The upper unit (UpU)*

628 The previous erosive stage generated a severely degraded and irregular landscape, somewhat
629 similar to the Pre-LwU, but without the complete disappearance of the former slope
630 accumulations. In the general evolutionary model established by Peña-Monné et al. (2005), the
631 normal trend is for new accumulations of the UpU to progressively substitute the LwU. This is
632 the most frequent situation observed in all previous works on Holocene slopes. However, Peña
633 Enroque has a different arrangement of the slopes: the UpU is superimposed on the LwU in
634 many areas (sections 1, 3, 5, 6 and 7). This circumstance has very positive consequences for
635 the study of the evolutionary stages of the slope, because the LwU and its paleosol are
636 preserved almost intact (Figure 8).

637 This second stage of slope regularisation differs from the LwU. The morphology of the new
638 slopes is steeper (30-35°), begins at the foot of the limestone escarpment, and has a concave
639 profile that connects with nearby valleys. We can observe this stage as an independent
640 landform in the N, S and SE of Peña Enroque (Figure 2).

641 The composition of the UpU shows a prevalence of thick sediments, even including boulders
642 and cobbles. It is a debris-covered and gravity-controlled slope with rock falls, washing of fine
643 materials, localised fluxes, and ploughing blocks, etc. These materials and processes fit in a
644 dynamic of limestone escarpment retreat and transport by means of surface run-off and
645 generation of debris fans in a steep slope setting. The final result is regularisation, but not as
646 complete as it was the LwU. Now the slopes have two sectors with morphologies that are clearly
647 separated: an almost vertical escarpment and a concave or rectilinear talus (Figure 7, 4).

648 The basal part of the UpU sometimes has an almost rectilinear contact with the LwU (sections
649 5, 6 and 7), without large or deep channels separating them. However, in some cases (section

650 1) this contact is more irregular because of small fluxes that introduced materials from the
651 paleosol of LwU into the the UpU.

652 Inside the accumulation of the UpU there are at least two moments of increased stability
653 indicated by the development of two paleosols with A-horizons (IIA and IA_h, levels 2b and 2d in
654 Section 6, respectively) that break the accumulative dynamic (Figure 5, section 6, and Figure 8).
655 Horizon IA_h is considered a paleosol and not the current active soil because it is being cut by
656 the existing erosive slope profile (Figure 8). These two paleosols were quickly generated
657 without time to develop B horizons and in the case of IA_h almost without any washing of salts.
658 The short time duration of these sub-stages of the UpU is confirmed by the chronology obtained
659 in sections 6 and 7.

660 The only chronological elements for the UpU are five modern wheel-thrown pottery shards
661 recovered from the upper levels of this unit in section 7, providing a *post-quem terminus* for the
662 formation of the deposit. Their typology points to the 17th to 19th centuries and TL dating
663 performed on one of them precisely confirms that chronology to AD 1624 ± 21 (MADN-
664 5998BIN). This age for the UpU accumulation fits with the chronology of other slopes in nearby
665 areas of the Ebro Depression, such as the northern escarpment of the river Ebro at El Castellar
666 and Castillo de Miranda (Peña-Monné, 1996; Constante et al., 2010), in the Huesca Depression
667 (Rodríguez-Vidal, 1986), or in the lower courses of the Segre and Cinca Rivers (Peña-Monné et
668 al., 1988; Peña-Monné and González-Pérez, 1992; Peña-Monné et al., 1996; Peña-Monné and
669 González-Pérez, 2000). Therefore, we can assume that it is a generalised slope formation
670 stage in NE Spain. The climatic conditions that were necessary for its genesis imply an abrupt
671 change that contrasts with the previous stage characterised by erosive processes. However,
672 this new regularisation stage represented by the UpU was less important than the LwU.

673 There is only one climatic phase after the Medieval Climate Anomaly with the specific conditions
674 that could generate the UpU, that is, the LIA with its highly variable precipitation regime (Figure
675 9). In addition to the UpU, the LIA is also responsible for several aggradation stages in the
676 bottoms of the secondary valleys (Peña-Monné et al., 1993; Peña-Monné et al., 1996; Peña-
677 Monné et al., 2001; Peña-Monné et al., 2005; Constante et al., 2010) and important flood
678 episodes in the main courses of NE Spain (Llasat et al., 2005; Thorndycraft and Benito, 2006;
679 Benito et al., 2008) and Europe (Macklin et al., 2006). The wetter conditions of the LIA are also

680 evidenced by the palaeolimnological records in the western Mediterranean – Estanya and
681 Montcortés lakes (Corella et al., 2011b; Morellón et al., 2011) – in contrast with the eastern
682 Mediterranean that was dryer during this period (Roberts et al., 2008; Roberts et al., 2012).
683 The two sub-stages of the UpU represented by the horizons IAh and IIA show the
684 environmental variability of the LIA, which has been determined for the NE of Spain through
685 dendroclimatic studies (Saz-Sánchez, 2003) and Pyrenean glacial evolution (Chueca and
686 Julián, 1996). These types of paleoclimatic records, as well as other paleoclimatic records
687 (lacustrine and marine sequences, increased runoff, vegetation changes) enable the
688 determination for the Pyrenean region (Morellón et al., 2012) of two stages in the evolution of
689 LIA: the first with fluctuating moist conditions and relatively cold temperatures (ca. AD 1300-
690 1600); and the second with lower temperatures (glaciers advances), greater runoff, and more
691 humidity (ca. AD 1600-1800). This climatic information concurs with the data obtained from the
692 UpU in section 6. The pottery shard dated by means of TL in section 7 was placed slightly
693 above the horizon IIA. Therefore, the first LIA accumulation and later stabilisation took place
694 before the 17th century. During or after this century, the second accumulation arose (Figure 5,
695 section 6 level 2c, Table 3 C1 and C2 horizons) and so the accumulation could be related to the
696 cooler temperatures of the Maunder Minimum (AD 1640-1710). In NE Spain, dendroclimatic
697 data shows a series of dry anomalies (AD 1660-1670, 1680-1690, Saz-Sánchez, 2003) during
698 this second period. It is not until the end of the 19th century that we find a recovery of
699 precipitation (AD 1880-1890, Saz-Sánchez, 2003; Morellón et al., 2012) which can be linked to
700 the development of the IAh horizon. Its short temporal duration and its proximity to present day
701 dry conditions concur with the poor development of this paleosol as evidenced by the
702 edaphological data. These stages during the LIA are concurrent with the successive solar
703 irradiance minimums described by Steinhilber et al. (2012) by means of different proxy data.

704

705 *Present dynamics*

706 In recent and present times, the prevailing processes in these slopes are mainly incisions in the
707 UpU unit. In those areas where both units are superimposed (sections 1, 5, 6 and 7) the
708 incisions cut through the whole of the accumulation. These gullies have a radial course from the

709 base line of the limestone escarpment towards the nearby flat fields and they generate talus
710 flatirons morphologies in the slopes (Figure 7, 5) and alluvial fans in the distal segment.
711 The upper surface of the UpU suffers an intense washing of fine grain material, leaving a stony
712 pavement that truncates its original topography, mainly affecting the most superficial paleosol
713 horizon IAh (Figure 8). In addition, there are small flux processes and ploughing blocks in the
714 NW slope, which is wetter than the SE side. In the dryer slopes rock falls of large blocks spread
715 chaotically over the surface of the UpU creating a debris-covered slope (Figure 6).
716 From the second half of the 19th century, climate conditions favoured the dynamism of the
717 abovementioned processes. Continental Mediterranean climate has few, but very intense
718 precipitations, that are especially erosive during the summer. Despite a recent decline in
719 anthropic land use pressure, the intense degradation of the natural environment caused by
720 several centuries of overgrazing on the slopes and the soft local lithologies (gypsum, clay and
721 marl) further promoted erosive processes because they prevented vegetation recovery.
722 The erosion also affects archaeological sites, even the most recent sites, such as medieval and
723 modern castles. A great part of the archaeological record is currently interpretable and
724 understandable through the remains contained in slope accumulations, as is the case of Peña
725 Enroque. Therefore, it is urgent to study the archaeological materials in these secondary
726 contexts using geoarchaeological criteria and methods to obtain as much archaeological and
727 paleoenvironmental information as possible.

728

729

730 **Conclusions**

731 The information obtained through the geomorphological and geoarchaeological study of Peña
732 Enroque enables us to make more precise descriptions of some aspects of the Holocene slope
733 system in NE Spain. The newly available data places the date of the beginning of the LwU
734 accumulation in the late Chalcolithic. The paleosol that culminates the long slope stability period
735 reaches Ibero-Roman times. This implies that the paleoenvironmental conditions of the central
736 sector of the Ebro Depression allowed the development of soils until that period. Afterwards, an
737 accelerated degradation of soils began as a result of the intensification of the anthropic
738 activities, especially from the late Roman period, as revealed by the sedimentary infills in

739 nearby secondary valleys (Peña-Monné et al., 2004). The resulting erosion is responsible for
740 the almost complete disappearance of the LwU. However, in Peña Enroque this unit was
741 fortunately preserved and fossilised under the new slope accumulation (UpU), whose upper
742 levels are dated to the second half of the LIA (17th-19th century). This second great moment of
743 slope activity had at least two stabilisation periods that allowed the development of two soils
744 which have now been eroded. The UpU is important for evaluating the incidence of LIA in lower
745 areas of the Mediterranean. The LIA caused specific morphologies (quite different to those of
746 the LwU) that are currently still active.

747 Finally, in summary we outline the evolutionary stages of the Upper Holocene in the NE of
748 Spain (Figure 9), according to the new data recovered from the Peña Enroque study and
749 previous paleoenvironmental works:

750

- 751 1. Pre-lower unit stage (Pre-LwU): chrono-culturally concurs with the Chalcolithic. Its
752 environmental conditions were arid or semiarid. The landscape was characterised by a
753 prevalence of badlands. It can be related to the 4.2 event of Bond et al. (Bond et al.,
754 1997) or the RCC 3 (4200-3800 BP) of Mayewski et al. (2004) and with an aridification
755 phase identified by Jalut et al. (2000).
- 756 2. Lower unit (LwU) slope accumulation stage: began in the late Chalcolithic and
757 continued during the Bronze and Iron Ages. Soil developed on top and reached at least
758 the 2nd century BC. Climatic conditions for this stage were cooler and wetter, generating
759 solifluxion processes. This stage matches event 2.8 of Bond et al. (Bond et al., 1997)
760 and the RCC 4 (3500-2500 BP) of Mayewski et al. (2004).
- 761 3. Intermediate erosive stage (Inter LwU-UpU): spans from the late Roman Period to post-
762 Medieval times. Most of the LwU was eroded during this stage – caused by an
763 aridification of the climate and anthropic pressure on the vegetal cover. During this
764 period, Jalut et al. (2000) indicates two aridification phases that happen in a warm
765 global context.
- 766 4. Upper unit (UpU) slope accumulation stage: concurs with the LIA. New accumulations
767 regularised the previously eroded slopes. However, it locally covered the remains of the

768 LwU. In this unit there are two cycles of aggradation-stabilisation that correspond with
769 climatic sub-stages of the LIA.
770 5. Present day incision stage: the consequence of the combination of climate conditions
771 favourable to erosion and recent-present anthropic pressure on the environment. All of
772 the remains of the accumulation units are being eroded and this is severely affecting the
773 archaeological record.

774

775

776 **Acknowledgments**

777 This work is a contribution of the Quaternary Paleoenvironments Research Group (PALEOQ)
778 and *Primeros Pobladores del Valle del Ebro* Research Group (PPVE), both partners of the
779 Institute of Environmental Sciences (IUCA), University of Zaragoza – Aragon Regional
780 Government.

781 Funding for this study was made available by the *Secretaría de Políticas Universitarias del*
782 *Ministerio de Educación* (Argentina) and the I+D+i project *Dinámica de la ocupación*
783 *prehistórica del valle medio Ebro durante el Holoceno Superior* (HAR2012-36967, *Ministerio de*
784 *Economía y Competitividad, Spanish Government*).

785 We wish to thank Dr. Penélope González-Sampérez for her collaboration in the palynological
786 analyses, despite the lack of positive results.

787 We are grateful to the reviewers of this paper for their comments and corrections. However, any
788 mistake or misinterpretation found in the text is authors only responsibility.

789

790

791 **References cited**

- 792 Aitken, M.J. (1985), *Thermoluminescence Dating*, Academy Press, London, 359 pp.
793 Arauzo, T., Gutiérrez-Elorza, M., and Sancho-Marcén, C. 1996. Facetas triangulares de ladera
794 como indicadores paleoclimáticos en ambientes semiáridos. *Depresión del Ebro*.
795 *Geogaceta*, 20, 1093-1095.
796 Arribas, J.G.; Millán, A.; Sibilia, E.; Calderón, T. (1990), "Factores que afectan a la
797 determinación del error asociado a la datación absoluta por TL: Fabrica de ladrillos".
798 *Bol. Soc. Es. De Min.* 13, 141-147.
799 Badía-Villas, D., Martí, C., Palacio, E., Sancho, C., and Poch, R. M. 2009. Soil evolution over
800 the Quaternary period in a semiarid climate (Segre river terraces, northeast Spain).
801 *Catena*, 77, 165-174.
802 Baize, D. And Girard, M.-C. (Coord.) 2009. *Référentiel Pédologique 2008*, Ass. Fr. Étude du
803 Sol, Quae Ed. Paris. 405 p.

- 804 Bea-Martínez, M., Domingo, R., Pérez-Lambán, F., Reklaityte, I., and Uribe, P. 2011.
805 Prospecciones arqueológicas en el término municipal de La Muela. *Salduie*, 10.
- 806 Benito, G., V.R., T., M., R., Sánchez-Moya, Y., and Sopena, A. 2008. Palaeoflood and
807 floodplain records from Spain: Evidence for long-term climate variability and
808 environmental changes. *Geomorphology*(101), 68-77.
- 809 Bintliff, J. L. 1982. Paleoclimatic modelling of environmental changes in the East mediterranean
810 region since the last glaciation. In: J. L. Bintliff, and W. Van Zeist, (Eds.) *Paleoclimates,*
811 *Paleoenvironments and Human Communities in the Eastern Mediterranean Region in*
812 *Later Prehistory.* BAR Int. Ser., pp. 485-527.
- 813 Bond, G., Showers, W., Cheseby, M., Lotti, R., Almasi, P., deMenocal, P., Priore, P., Cullen, H.,
814 Hajdas, I., and Bonani, G. 1997. A Pervasive Millennial-Scale Cycle in North Atlantic
815 Holocene and Glacial Climates. *Science*, 278, 1257-1266.
- 816 Boroda, R., Amit, R., Matmon, A., Team, A., Finkel, R., Porat, N., Enzel, Y., and Eyal, Y. 2011.
817 Quaternary-scale evolution of sequences of talus flatirons in the hyperarid Negev.
818 *Geomorphology*, 127, 41-52.
- 819 Branch, N. P., Kemp, R. A., Silva, B., Meddens, F. M., Williams, A., Kendall, A., and
820 Pomacanchiari, C. V. 2007. Testing the sustainability and sensibility to climatic change
821 of terrace agricultural systems in the Peruvian Andes: a pilot study. *Journal of*
822 *Archaeological Science*, 34, 1-9.
- 823 Burillo, F., Gutiérrez-Elorza, M., and Peña-Monné, J. L. 1981a. El cerro del castillo de Alfambra
824 (Teruel). Estudio interdisciplinar de Geomorfología y Arqueología. *Kalathos*, 1, 7-63.
- 825 Burillo, F., Gutiérrez-Elorza, M., and Peña-Monné, J. L. 1981b. Las vertientes del cerro del
826 castillo de Alfambra (Teruel)(Eds.) *Actas V Reunión Nacional del Grupo Español de*
827 *Trabajo del Cuaternario*, Sevilla, pp. 231-244.
- 828 Burillo, F., Gutiérrez-Elorza, M., and Peña-Monné, J. L. 1983. La Geoarqueología como ciencia
829 auxiliar. Una aplicación a la Cordillera Ibérica Turolense. *Revista de Arqueología*, 26, 6-
830 13.
- 831 Constante, A., Dossche, R., Peña-Monné, J. L., Sancho-Marcén, C., and De Dapper, M. 2009.
832 Holocene Evolution and Geoarchaeology in the Ebro Valley around Zaragoza
833 (Northern Spain). In: M. De Dapper, F. Vermeulen, S. Deprez, and D. Taelman, (Eds.)
834 *Ol'man river Geo-archaeological aspects of rivers and river plains.* Akademia Press,
835 Ghent, pp. 241-256.
- 836 Constante, A., and Peña-Monné, J. L. 2009. Human-induced erosion and sedimentation during
837 the Holocene in the central Ebro depression, Spain, Congreso Internacional sobre
838 Desertificación 2009. Universidad de Murcia, Murcia, pp. 207-210.
- 839 Constante, A., Peña-Monné, J. L., and Muñoz, A. 2010. Alluvial geoarchaeology of an
840 ephemeral stream: Implications for Holocene landscape change in the Central part of
841 the Ebro Depression, Northeast Spain. *Geoarchaeology*, 25 (4), 475-496.
- 842 Constante, A. 2011. Estudio geoarqueológico de los registros holocenos del sector central del
843 valle del Ebro. Tesis Doctoral, Universidad de Zaragoza, Dpto. de Geografía y
844 Ordenación del Territorio, Zaragoza.
- 845 Constante, A., Peña-Monné, J. L., Muñoz, A., and Picazo, J. V. 2011. Climate and
846 anthropogenic factors affecting alluvial fan development during the late Holocene in the
847 central Ebro Valley, northeast Spain. *The Holocene*, 21, 275–286.
- 848 Corella, J. P., Amrani, A., Sigró, J., Morellón, M., Rico, E., and Valero-Garcés, B. 2011a. Recent
849 evolution of Lake Arreo, northern Spain: influences of land use change and climate.
850 *Journal of Paleolimnology*, 46, 469–485.
- 851 Corella, J. P., Valero-Garcés, B., Moreno, A., Morellón, M., Rull, V., Giralt, S., Rico, M. T., and
852 Pérez-Sanz, A. 2011b. Climate and human impact on a meromictic lake during the last
853 6000 years (Montcortès Lake, Central Pyrenees, Spain). *Journal of Paleolimnology*, 46,
854 351–367.
- 855 Cuadrat, J. M., Saz Sánchez, M. Á., and Vicente Serrano, S. M. 2007. Atlas climático de
856 Aragón. Gobierno de Aragón, Zaragoza, pp.
- 857 Chueca, J., and Julián, A. 1996. Datación de depósitos morrénicos de la Pequeña Edad del
858 Hielo: Macizo de la Maladeta. In: A. Perez-Alberti, I. P. Martín, W. Chesworth, and A.
859 Martínez-Cortizas, (Eds.) *Dinámica y evolución de medios cuaternarios.* Xunta de
860 Galicia, Santiago de Compostela, pp. 171-182.
- 861 Eidt, R. C. 1977. Detection and examination of anthrosols by phosphate analysis. *Science*, 197,
862 1327-1333.

- 863 Fleming, S.J. (1970), "Thermoluminescence Dating Refinement of Quartz inclusion Method",
864 *Archaeometry* 12, 13-30.
- 865 García-Ruiz, J. M.; Martí-Bono, C.; Valero, B.; González-Samperiz, P.; Lorente, A.; Beguería,
866 S.; Edwards, L. 2000. Derrubios de ladera en el Pirineo Central español: significación
867 cronológica y paleoclimática. In: J.L. Peña-Monné; M. Sánchez-Fabre and M.V. Lozano
868 (Eds.). *Procesos y formas periglaciares en la montaña mediterránea*, I.E.T., Teruel, 63-
869 79.
- 870 Gerson, R. 1982. Talus relict in deserts: a key to major climatic fluctuations. *Israel Journal Earth*
871 *Science*, 31, 123-132.
- 872 Gribbin, J., and Lamb, H. H. 1978. Climatic change in historical times. In: J. Gribbin, (Eds.)
873 *Climatic Change*. Cambridge University Press, pp. 68–82.
- 874 Gutiérrez-Elorza, M., and Peña-Monné, J. L. 1989. Upper Holocene climatic change and
875 geomorphological processes on slopes and infilled valleys from archeological dating
876 NE-Spain. In: M. M. Boer, and F. A. Eybergen, *Landscape Ecological Impact of Climate*
877 *Change: proceedings of a European conference*. Dutch Ministry of the Environment,
878 Lunteren, The Netherlands, pp. 21.
- 879 Gutiérrez-Elorza, M., and Peña-Monné, J. L. 1992. Evolución climática y geomorfológica del
880 Holoceno superior (Cordillera Ibérica, Depresión del Ebro y Pre-Pirineo). In: A.
881 Cearreta, and F. M. Ugarte, (Eds.) *The Late Quaternary in the Western Pyrenean*
882 *Region*. Universidad del País Vasco, pp. 109-124.
- 883 Gutiérrez-Elorza, M., and Peña-Monné, J. L. 1998. Geomorphology and Late Holocene Climatic
884 Change in Northeastern Spain. *Geomorphology*, 23, 205-217.
- 885 Gutiérrez-Elorza, M., Sancho-Marcén, C., and Arauzo, T. 1998a. Scarp retreat in semiarid
886 environments from talus flatirons (Ebro Basin). *Geomorphology*, 25, 111-121.
- 887 Gutiérrez-Elorza, M., Sancho-Marcén, C., Arauzo, T., and Peña-Monné, J. L. 1998b. Evolution
888 and paleoclimatic meaning of the talus flatirons in the Ebro Basin, northeast Spain. In:
889 A. S. Alsharham, K. W. Glennie, G. L. Whittle, and C. G. S. C. Kendall, (Eds.)
890 *Quaternary Deserts and Climatic Change*. Balkema, Rotterdam, pp. 593-599.
- 891 Gutiérrez-Elorza, M., Gutiérrez, F., and Desir, G. 2006. Considerations on the chronological and
892 causal relationship between talus flatirons and palaeoclimatic changes in central and
893 northeast Spain. *Geomorphology*, 73, 50-63.
- 894 Gutiérrez-Elorza, M., Lucha, P., Gutiérrez, F., Moreno, A., Guerrero, J., Martín-Serrano, A.,
895 Nzal, F., Desir, G., Marín, C., and Bonachea, J. 2010. Are talus flatiron sequences in
896 Spain climate-controlled landforms? *Zeitschrift für Geomorphologie*, 54 (2), 243-252.
- 897 Gutiérrez, F., Valero-Garcés, B., Desir, G., González-Sampériz, P., Gutiérrez-Elorza, M.,
898 Linares, R., Zarroca, M., Moreno, A., Guerrero, J., Roqué, C., Arnold, L. J., and
899 Demuro, M. 2012 (in press). Late Holocene evolution of playa lakes in the central Ebro
900 depression based on geophysical surveys and morpho-stratigraphic analysis of
901 lacustrine terraces. *Geomorphology*, 1-21.
- 902 IUSS. 2007. World Reference Base for Soil Resources, World Soil Resources Reports. FAO,
903 Rome, pp.
- 904 Jalut, G., Esteban, A., Bonnet, L., Gauquelin, T., and Fontugne, M. 2000. Holocene climatic
905 changes in the western Mediterranean, from south-east France to south-east Spain.
906 *Palaeogeography, Palaeoclimatology, Palaeoecology*, 160, 255-290.
- 907 Lamb, H. 1977. *Climate: Present, Past and Future*. Vol. 2. *Climatic History and the Future*.
908 Methuen.
- 909 Leonardi, G., Miglavacca, M., and Nardi, S. 1999. Soil phosphorous analysis as an integrative
910 tool for recognizing buried ancient ploughsoils. *Journal of Archaeological Science*, 26,
911 343-352.
- 912 Llasat, M. C., Barriendos, M., Barrera, A., and Rigo, T. 2005. Floods in Catalonia (NE Spain)
913 since the 14th century. Climatological and meteorological aspects from historical
914 documentary sources and old instrumental records. *Journal of Hydrology*, 313, 32-47.
- 915 Maasch, K. A., Mayewski, P. A., Rohling, E. J., Stager, J. C., Karlén, W., Meeker, L. D., and
916 Meyerson, E. A. 2005. A 2000-year context for modern climate change. *Geogr. Ann.*, 87
917 (A(1)), 7-15.1.
- 918 Macklin, M. G., Benito, G., Gregory, K. J., Johnstone, E., Lewin, J., Michczyn´ska, D. J., Soja,
919 R., Starkel, L., and Thorndycraft, V. R. 2006. Past hydrological events reflected in the
920 Holocene fluvial record of Europe. *Catena*, 66, 145-154.
- 921 Mayewski, P. A., Rohling, E. E., Stager, J. C., Karlén, W., Maasch, K. A., Meeker, L. D.,
922 Meyerson, E. A., Gasse, F., Kreveld, S. v., Holmgren, K., Lee-Thorp, J., Rosqvist, G.,

- 923 Rack, F., Staubwasser, M., Schneider, R. R., and Steig, E. J. 2004. Holocene climate
924 variability. *Quaternary Research*, 62 (3), 243-255.
- 925 Morellón, M., Valero-Garcés, B., González-Sampériz, P., Vegas-Vilarrúbia, T., Rubio, E.,
926 Rieradevall, M., Delgado-Huertas, A., Mata, P., Romero, Ó., Engstrom, D. R., López-
927 Vicente, M., Navas, A., and Soto, J. 2011. Climate changes and human activities
928 recorded in the sediments of Lake Estanya (NE Spain) during the Medieval Warm
929 Period and Little Ice Age. *Journal of Paleolimnology*, 46, 423–452.
- 930 Morellón, M., Pérez-Sanz, A., Corella, J. P., Büntgen, U., Catalán, J., González-Sampériz, P.,
931 González-Trueba, J. J., López-Sáez, J. A., Moreno, A., Pla-Rabes, S., Saz-Sánchez, M.
932 Á., Scussolini, P., Serrano, E., Steinhilber, F., Stefanova, V., Vegas-Vilarrúbia, T., and
933 Valero-Garcés, B. 2012. A multi-proxy perspective on millennium-long climate variability
934 in the Southern Pyrenees. *Climate of the Past*, 8, 683-700.
- 935 Moreno, A., Pérez, A., Frigola, J., Nieto-Moreno, V., Rodrigo-Gámiz, M., González-Sampériz,
936 P., Morellón, M., Martín-Puertas, C., Corella, J. P., Belmonte, Á., Sancho, C., Cacho, I.,
937 Herrera, G., Canals, M., Jiménez-Espejo, F., Martínez-Ruiz, F., Vegas, T., and Valero-
938 Garcés, B. 2012. The Medieval Climate Anomaly in the Iberian Peninsula reconstructed
939 from marine and lake records. *Quaternary Science Reviews*, 43, 16-32.
- 940 Nambi, S.V.; Aitken, M.J. (1986), "Annual dose conversion factors for TL and ESR dating",
941 *Archaeometry* 28, 202-205.
- 942 Nelson, R. E., and Sommers, L. E. 1982. Total carbon and organic matter. In: A. L. Page, R. H.
943 Miller, and D. R. Keeney, (Eds.) *Methods of Soil Analysis. Part 2: Chemical and*
944 *Microbiological Properties*. American Society of Agronomy, Madison, Wisconsin, pp.
945 539-557.
- 946 Nemeç, W.; Kazancı, N. 1999. Quaternary colluvium in west-central Anatolia: sedimentary
947 facies and palaeoclimatic significance. *Sedimentology*, 46, 139-170.
- 948 Peña-Monné, J. L. 1983. Dinámica reciente de vertientes en el valle medio del Segre (zona de
949 Anya-Artesa de Segre, prov. de Lérida)(Eds.) *Actas del VIII Coloquio de Geografía*,
950 Barcelona, pp. 123-130.
- 951 Peña-Monné, J. L., González-Pérez, J. R., and Rodríguez, J. I. 1988. Estudi gearqueològic del
952 Tossal de Moradilla (Lleida). *Recerques Terres de Ponent*, IX, 31-41.
- 953 Peña-Monné, J. L., Julián, A., and Chueca, J. 1991. Sequèncs evolutives des accumulations
954 holocenes à la hoya de Huesca dans le contexte general du Bassin de l'Ebre
955 (Espagne). *Physio-Géo*, 22-23, 55-60.
- 956 Peña-Monné, J. L., and González-Pérez, J. R. 1992. Hipòtesis evolutiva de los cambios en la
957 dinámica geomorfológica del Baix Cinca y Segre (Depresión del Ebro) durante el
958 Pleistoceno superior-Holoceno a partir de los datos gearqueológicos. *Cuaternario y*
959 *Geomorfología*, 6, 103-110.
- 960 Peña-Monné, J. L., and Rodanés, J. M. 1992. Evolución geomorfológica y ocupación humana
961 en el cerro de Masada de Ratón (Baix Cinca, prov. de Huesca). *Cuaternario y*
962 *Geomorfología*, 6, 81-89.
- 963 Peña-Monné, J. L., Echeverría, M. T., Petit-Maire, N., and Lafont, R. 1993. Cronología e
964 interpretación de las acumulaciones holocenas de la val de Las Lenas (Depresión del
965 Ebro, Zaragoza). *Geographicalia*, 30, 321-332.
- 966 Peña-Monné, J. L. 1996. Los valles holocenos del escarpe de yesos de Juslibol (sector central
967 de la depresión del Ebro): Aspectos geomorfológicos y gearqueológicos. *Arqueología*
968 *Espacial*, 15, 83-102.
- 969 Peña-Monné, J. L., González-Pérez, J. R., and Rodríguez, J. I. 1996. Paleoambientes y
970 evolución geomorfológica en yacimientos arqueológicos del sector oriental de la
971 depresión del Ebro durante el Holoceno superior. In: A. Pérez Alberti, P. Martini, W.
972 Chesworth, and A. Martínez Cortizas, (Eds.) *Dinámica y evolución de medios*
973 *cuaternarios*, Santiago, pp. 63-80.
- 974 Peña-Monné, J. L., and González-Pérez, J. R. 2000. Evolució dels abrics de gres de la vall
975 mitjana del riu Segre (sector oriental de la Depressió de l'Ebre). *Gearqueologia i*
976 *Quaternari litoral*. Memorial M.P. Fumanal, 217-227.
- 977 Peña-Monné, J. L., Echeverría, M. T., Chueca, J., and Julián, A. 2001. Processus
978 géomorphologiques d'accumulation et incision pendant l'Antiquité Classique et ses
979 rapport avec l'activité humaine et les changements climatiques holocènes dans la
980 vallée de la Huerva (Bassin de l'Ebre, Espagne). In: F. Vermeulen, and M. De Dapper,
981 (Eds.) *Geoarchaeology of the Landscapes of Classical Antiquity*. Peeters, Leuven, pp.
982 151-159.

- 983 Peña-Monné, J. L., Rubio-Fernández, V., González-Pérez, J. R., and Vázquez, P. 2002.
984 Cambios dinámicos en laderas holocenas del valle del Segre (Depresión del Ebro). In:
985 L. A. Longares Aladrén, and J. L. Peña-Monné, (Eds.) Aportaciones Geográficas en
986 memoria del Prof. L. Miguel Yetano. Universidad de Zaragoza, Zaragoza, pp. 421-432.
- 987 Peña-Monné, J. L., Julián, A., Chueca, J., Echeverría, M. T., and Ángeles, G. R. 2004. Etapas
988 de evolución holocena en el valle del río Huerva: Geomorfología y Geoarqueología. In:
989 J. L. Peña-Monné, L. A. Longares, and M. Sánchez-Fabre, (Eds.) Geografía Física de
990 Aragón. Aspectos generales y temáticos. Universidad de Zaragoza e Institución
991 Fernando el Católico, Zaragoza, pp. 289-302.
- 992 Peña-Monné, J. L., Rubio-Fernández, V., and González-Pérez, J. R. 2005. Aplicación de
993 modelos geomorfológicos evolutivos al estudio de yacimientos arqueológicos en
994 medios semiáridos (Depresión del Ebro, España)(Eds.) A Geografía ibérica no contexto
995 europeo (X Coloquio Ibérico de Geografía, 22-24 de Setembro de 2005). Universidade
996 de Evora.
- 997 Pérez-Lambán, F., Fanlo-Loras, J., and Picazo-Millán, J. V. 2011. El poblamiento antiguo en el
998 valle del río Huerva. Resultados de las campañas de prospección de 2007-2009.
999 Salduie, 10.
- 1000 Picazo-Millán, J. V., and Perales-García, M. P. 1994. Informe de la actuación arqueológica
1001 realizada en la ladera SO del Castillo (Alfambra, Teruel)(Eds.) Arqueología Aragonesa,
1002 1991. Diputación General de Aragón, Departamento de Educación y Cultura, Zaragoza.
- 1003 Picazo-Millán, J. V. 1999-2000. Nuevas dataciones para la Edad Media del Bronce en la
1004 cuenca del río Alfambra (Teruel). *Kalathos*, 18-19, 7-26.
- 1005 Reimer, P. J., Baillie, M. G. L., Bard, E., Bayliss, A., Beck, J. W., Blackwell, P. G., Bronk
1006 Ramsey, C., Buck, C. E., Burr, G. S., Edwards, R. L., Friedrich, M., Grootes, P. M.,
1007 Guilderson, T. P., Hajdas, I., Heaton, T. J., Hogg, A. G., Hughen, K. A., Kaiser, K. F.,
1008 Kromer, B., McCormac, F. G., Manning, S. W., Reimer, R. W., Richards, D. A.,
1009 Southon, J. R., Talamo, S., Turney, C. S. M., van der Plicht, J., and Weyhenmeyer, C.
1010 E. 2009. IntCal09 and Marine09 radiocarbon age calibration curves, 0–50, 000 years
1011 cal BP. *Radiocarbon*, 51, 1111-1150.
- 1012 Rhoades, J. D. 1982. Soluble salts. In: A. L. Page, R. H. Miller, and D. R. Keeney, (Eds.)
1013 *Methods of Soil Analysis. Part 2: Chemical and Microbiological Properties*. American
1014 Society of Agronomy, Madison, Wisconsin, pp. 167-180.
- 1015 Roberts, N., Jones, M. D., Benkaddour, A., Eastwood, W. J., Filippi, M. L., Frogley, M. R.,
1016 Lamb, H. F., Leng, M. J., Reed, J. M., Stein, M., Stevens, L., Valero-Garcés, B., and G.,
1017 Z. 2008. Stable isotope records of Late Quaternary climate and hydrology from
1018 Mediterranean lakes: the ISOMED synthesis. *Quaternary Science Reviews*, 27, 2426-
1019 2441.
- 1020 Roberts, N., Moreno, A., Valero-Garcés, B., Corella, J. P., Jones, M., Allcock, S., Woodbridge,
1021 J., Morellón, M., Luterbacher, J., Xoplaki, E., and Türkeş, M. 2012. Palaeolimnological
1022 evidence for an east-west climate see-saw in the Mediterranean since AD 900. *Global
1023 and Planetary Change*, 84–85, 23–24.
- 1024 Rodanés, J. M., and Picazo-Millán, J. V. 2009. La cabaña mesolítica del Cabezo de la Cruz (La
1025 Muela, Zaragoza). In: P. Utrilla, and L. Montes (Eds.) *El Mesolítico Geométrico en la
1026 Península Ibérica*. Universidad de Zaragoza, Zaragoza, pp. 327-342.
- 1027 Rodríguez-Vidal, J. 1986. Geomorfología de las Sierras Exteriores oscenses y su piedemonte.
1028 Instituto de Estudios Altoaragoneses, Huesca.
- 1029 Roldán, J., Sampietro, M. M., Neder, L., and Vattuone, M. A. 2008. Efectos antrópicos de uso
1030 de suelos durante el Formativo en el Valle de Tafí (Tucumán, Argentina). *Chungara,
1031 Revista de Antropología Chilena*, 40 (2), 161-172.
- 1032 Rovira i Port, J. 2006. Las producciones cerámicas con impronta basal de estera vegetal del
1033 calcolítico final-bronze antiguo/medio de la península Ibérica. Acerca de la alternancia
1034 de influjos y el origen del protourbanismo en la depresión central catalana como
1035 modelo de territorio basculante. *Quaderns de prehistòria i arqueologia de Castelló*, 25,
1036 109-137.
- 1037 Royo-Guillén, J. I., Rey-Lanaspa, J., and Gómez-Lecumberri, F. 1997. El yacimiento
1038 campaniforme de Peñarroya. Jaulín (Zaragoza)(Eds.) *Arqueología Aragonesa 1993*.
1039 Diputación General de Aragón, Zaragoza, pp. 37-44.
- 1040 Sampietro, M. M., Roldán, J., Neder, L., Maldonado, M. G., and Vattuone, M. A. 2011.
1041 Formative pre-Hispanic agricultural soils in northwest Argentina. *Quaternary Research*,
1042 75 (1), 36-44.

- 1043 Sancho-Marcén, C., Peña-Monné, J. L., Muñoz, A., G., B., McDonald, E., Rhodes, E., and
 1044 Longares, L. A. 2008. Holocene alluvial morphosedimentary record and environmental
 1045 changes in the Bardenas Reales Natural Park (NE Spain). *Catena*, 73, 225-238.
- 1046 Sancho-Marcén, C., Gutiérrez-Elorza, M., Peña-Monné, J. L., and Burillo Mozota, F. 1988. A
 1047 quantitative approach to scarp retreat starting from triangular slope facets (Central Ebro
 1048 Basin, Spain). In: A. M. Harvey, and M. Sala, (Eds.) *Geomorphic Processes*, vol. II:
 1049 *Geomorphic Systems*. *Catena*, suppl. 13, pp. 139-146.
- 1050 Saz-Sánchez, M. Á. 2003. Temperaturas y precipitaciones en la mitad Norte de España desde
 1051 el s. XV. Estudio dendrocronológico. *Publicaciones del Consejo Protección de la*
 1052 *Naturaleza de Aragón, serie Investigación, Zaragoza*.
- 1053 Schlezinger, D. R., and Howes, B. L. 2000. Organic phosphorus and elemental ratios as
 1054 indicators of prehistoric human occupation. *Journal of Archaeological Science*, 27, 479–
 1055 492.
- 1056 Schmidt, K. H. 1988. Rates of scarp retreat: a means of dating neotectonic activity. In: V. H.
 1057 Jacobshagen, (Eds.) *The Atlas System of Morocco Studies on its Geodynamic*
 1058 *Evolution, Lecture Notes in Earth Science 15*, Berlin, pp. 445-462.
- 1059 Schmidt, K. H. 1989. Talus and pediment flatirons-erosional and depositional features of
 1060 dryland cuesta scarp. *Catena Suppl*, 14, 107-118.
- 1061 Schmidt, K. H. 1996. Talus and pediment flatirons-indicators of climatic change on scarp slope
 1062 on the Colorado Plateau, USA. *Zeitschrift für Geomorphologie*, 13 (Suppl), 135-158.
- 1063 Soil Survey Staff (SSS), 2010. *Keys to soil taxonomy*. 11th edition. USDA-Natural Resources
 1064 Conservation Service, Washington.
- 1065 Sopena, M. C. 1998. Estudio geoarqueológico de los yacimientos de la Edad del Bronce de la
 1066 comarca del Cinca medio (Huesca). Instituto de Estudios Altoaragoneses, Huesca.
- 1067 Steinhilber, F., Abreu, J. A., Beer, J., Brunner, I., Christl, M., Fischer, H., Heikkilä, U., Kubik,
 1068 P.W., Mann, M., McCracken, K.G., Miller, H., Miyahara, H., Oerter, H. and Wilhelms, F.
 1069 2012. 9,400 years of cosmic radiation and solar activity from ice cores and tree rings.
 1070 *Proceedings of the National Academy of Sciences*.
 1071 www.pnas.org/cgi/doi/10.1073/pnas.1118965109
- 1072 Stuiver, M., and Reimer, P. 1993. Extended 14C data base and revised CALIB 3.0 14C age
 1073 calibrating program. *Radiocarbon*, 35 (1), 215-230.
- 1074 Thorndycraft, V. R., and Benito, G. 2006. Late Holocene fluvial chronology of Spain: The role of
 1075 climatic variability and human impact. *Catena*, 66, 34-41.
- 1076 Van Geel, B., Buurman, J., and Waterbolk, H. T. 1996. Archaeological and palaeoecological
 1077 indications for an abrupt climate change in The Netherlands and evidence for
 1078 climatological teleconnections around 2650 BP. *Journal of Quaternary Science*, 11,
 1079 451-460.
- 1080 Van Steijn, H.; Bertran, P.; Francou, B.; Héту, B.; Texier, J.P. 1995. Models for the genetic and
 1081 environmental interpretation of stratified slope deposits: review. *Permafrost and*
 1082 *Periglacial Processes*, 6 (2), 125-146.
- 1083 Zimmerman, D.W. (1971), *Thermoluminescence Dating Using Fine Grain from Pottery*,
 1084 *Archaeometry* 13, 29-52.

1088 **List of tables**

1089 **Table 1.** TL dating of pottery shards from Peña Enroque.

1090 **Table 2.** ¹⁴C dating in slope units from Peña Enroque.

1091 **Table 3.** Soil main characteristics analysed in Section 6

1092

1093

1094 **List of figures**

1095 **Figure 1.** Situation and geomorphologic maps of Peña Enroque, with indication of the seven
1096 analysed sections and the location of the archaeological findings.

1097 **Figure 2.** NE panoramic view of the structural relief called Peña Enroque. Talus flatirons
1098 exposed in the photograph correspond to the upper unit of slope regularisation.

1099 **Figure 3.** Geomorphologic diagram of the northern slope of Peña Enroque that shows the two
1100 described units (lower and upper units), the main paleosol A-horizon, and the position of
1101 sections 1, 2 and 3. In the lower part of the figure there are three photographs of the sections
1102 with indications of their units and levels, dating samples and archaeological artefacts (see the
1103 text for further explanation).

1104 **Figure 4.** Geomorphologic diagram of the northern slope of Peña Enroque showing the two
1105 units (lower and upper units), the main paleosol A-horizon and the position of sections 4 and 5.
1106 In the lower part of the figure there are two photographs of the sections with indications of their
1107 units and levels, dating samples and archaeological artefacts (see the text for further
1108 explanation). In the upper part, drawings and photographs show some of the Bell Beaker
1109 pottery shards recovered from section 4 and surroundings.

1110 **Figure 5.** Geomorphologic diagram of the northern slope of Peña Enroque that shows the two
1111 described units (lower and upper units), the main paleosol A-horizon and the position of
1112 sections 6 and 7. In the lower part of the figure there are two photographs of the sections with
1113 indications of their units and levels, dating samples and archaeological artefacts (see the text
1114 for further explanation). In the upper part, drawings and photographs represent some of the
1115 Modern Age pottery shards recovered from Section 7 and surroundings.

1116 **Figure 6.** Photograph of the SE side of Peña Enroque showing the Miocene limestone
1117 escarpment and the slope of the upper unit. In the cut of the gully, the two superimposed units
1118 can be observed. A-horizons of the paleosols are indicated.

1119 **Figure 7.** Evolutionary diagrams showing the geomorphological state of Peña Enroque during
1120 different stages – from the Chalcolithic to the current morphology (2700 BC – AD 2013). The
1121 moments of aggradation of the two slope units are evidenced.

1122 **Figure 8.** Diagram synthesising the data obtained from the seven analysed sections. The
1123 arrangement of the two slope units, the paleosols, pottery position and chronological data are
1124 shown.

1125 **Figure 9.** Graph relating the described stability/incision slope stages to the climatic evolution of
1126 the late Holocene, the Bond et al. (1997) events, the Mayewski et al. (2004) RCCs, and the
1127 historical periods from the late Neolithic to the current time.
1128
1129

Table 1. TL dating of pottery shards from Peña Enroque.

References	Area & depth (m)	Material	TL age (yr from 2011)	Dates BC/AD	Cultural period
MADN-5995BIN	Summit (0.02)	Ceramic	3657 ± 250	1646 ± 250 BC	Bronze Age
MADN-5998BIN	Section 7 (0.15)	Ceramic	387 ± 21	AD 1624 ± 21	Modern Epoch

TL dating was done in the Laboratorio de Datación de la UAM (Universidad Autónoma de Madrid, Spain), following the methods proposed in Aitken (1985), Arribas et al. (1990), Fleming (1970), Nambi, S.V and Aitken, M.J. (1986), Zimmerman, D.W. (1971).

Table 2. ¹⁴C dating in slope units from Peña Enroque.

Laboratory Reference	Section number & depth (m)	Material	¹⁴ C yr BP	cal yr BP (2 σ ranges)	Cal yr BC (2 σ ranges)	Cultural period
GrA-45131	Section 4 (0.85)	Charcoal	3795 \pm 35	4346-4334 (0.8%) 4295-4083 (97.7%) 4029-4010 (1.5%)	2397-2385 (0.8%) 2346-2134 (97.6%) 2080-2067 (1.5%)	Late Chalcolithic
GrA-47554	Section 3 (2.05)	Charcoal	4015 \pm 40	4781-4769 (1.4%) 4607-4602 (0.5%) 4581-4413 (98.2%)	2832-2820 (1.4%) 2658-2653 (0.5%) 2632-2464 (98.2%)	Chalcolithic
GrA-50207	Section 5 (3.1)	Charcoal	4485 \pm 35	5295-5037 (95.3%) 5007-4979 (4.7%)	3346-3088 (95.3%) 3058-3030 (4.7%)	Early Chalcolithic
UZ-5952 / ETH-42556	Section 7 (0.95)	Charcoal	2110 \pm 30	2152-1995 (100%)	203-46 (100%)	Ibero-roman Epoch

Radiocarbon ages were calibrated to calendar ages by using **CALIB 6 (Stuiver and Reimer, 1993)** based on **Reimer et al. (2009)** calibration data set. Some conventional ¹⁴C dates have multiple intercepts in the calendar yr BP curve. Two-sigma calibrated age (BP and BC) is provided in ranges with indication of their relative area (in %) under 2 σ distribution. In bold most likely period.

Table 3. Soil main characteristics analysed in Section 6

Sample depth (cm)	Geom. Level	Edaf. Horizon	Munsell colour notation (dry; wet)	Gravels (% w/w)	Organic Matter (%)	C/N ratio	Total P (mg/kg)	CE (dS/m)	CaCO ₃ eq (%)	Texture
15	2d	IAh	7.5 YR 6/3; 7.5 YR 5/3	44.3	3.64	30.1	200	0.43	55.3	Clayey-skeletal
45	2c	IC1	7.5 YR 6.5/3; 5.5 YR 5.5/3	70.3	1.99	9.6	109	0.92	43.1	Clayey-skeletal
65		IC2	7.5 YR 6.5/3; 7.5 YR 5/3	57	1.48	4.5	144	2.92	61.3	Clayey-skeletal
100	2b	IIA	7.5 YR 6/3; 7.5 YR 5/3	39	4.63	17.9	198	0.75	37.0	Clayey-skeletal
120	2a	IIC1	7.5 YR 7/3; 7.5 YR 6/3	23	1.84	7.1	165	4.34	49.3	Clayey-skeletal
160		IIC2	7.5 YR 6.5/3; 7.5 YR 5/3	72*	2.03	9.0	151	nd	43.3	Clayey-skeletal
185	1b	IIIA	7.5 YR 5/2; 7.5 YR 4/2	35	4.00	18.0	279	0.34	34.5	Clayey
210	1a	IIIBw	7.5 YR 6.5/3; 7.5 YR 5/4	8	2.26	11.9	213	1.03	41.2	Loamy
270		IIIC1	7.5 YR 6.5/3; 7.5 YR 5/4	22	2.27	10.1	212	0.71	41.7	Clayey
330		IIIC2	7.5 YR 6.5/3; 7.5 YR 5/4	23	2.26	8.7	222	1.15	41.5	Clayey

Figure 1
[Click here to download high resolution image](#)

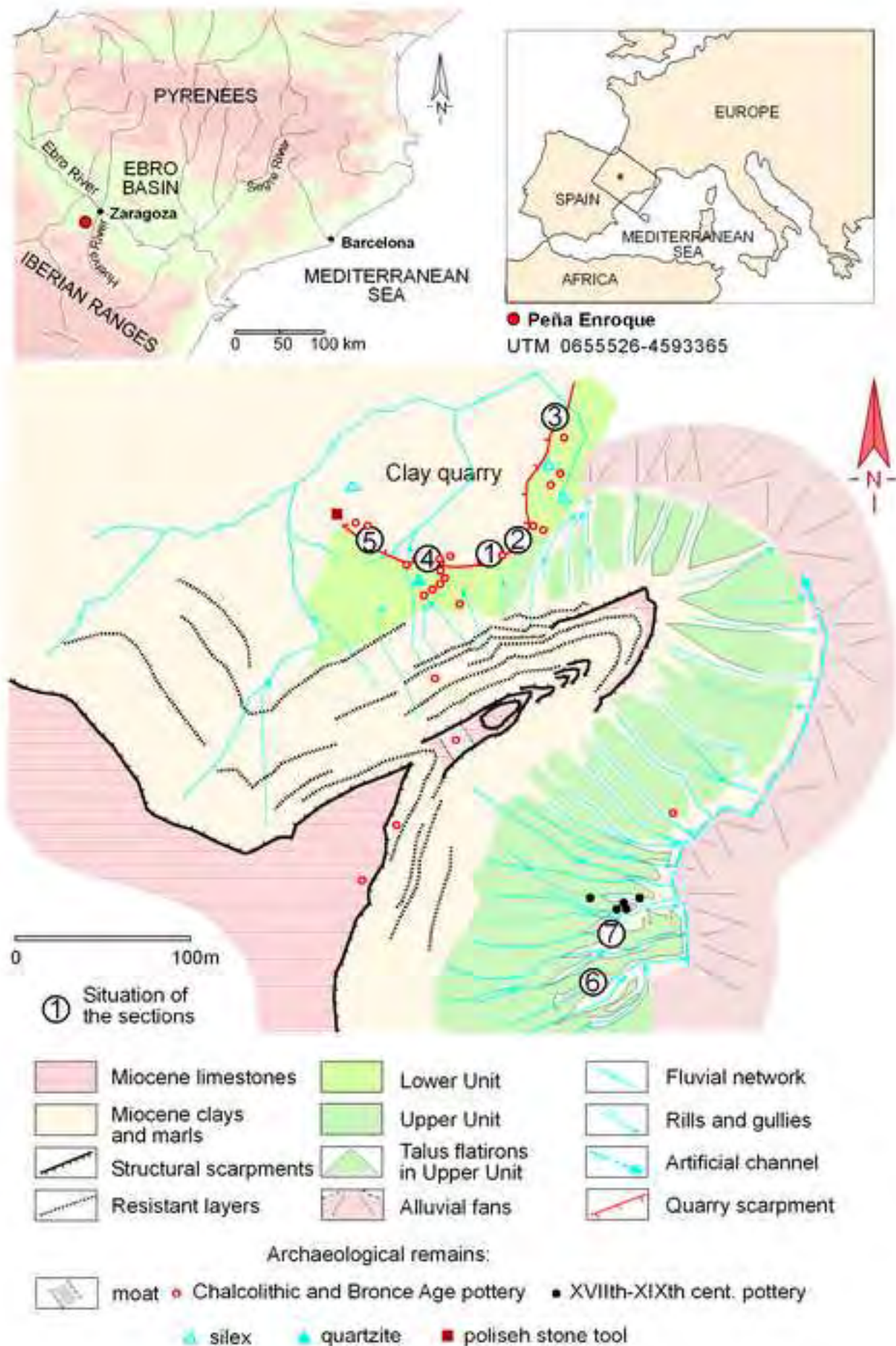


Figure 2
[Click here to download high resolution image](#)



Figure 3
[Click here to download high resolution image](#)

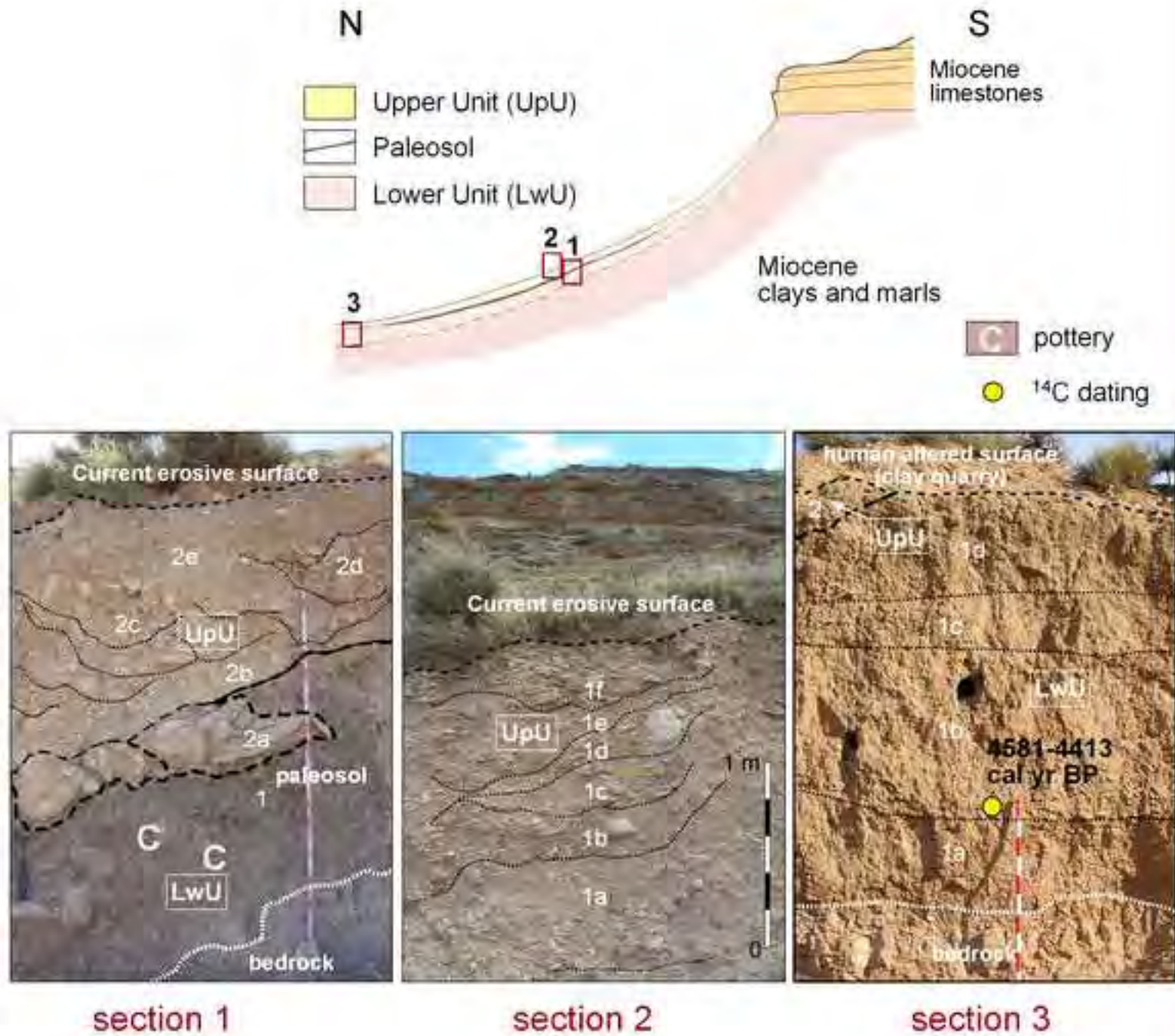
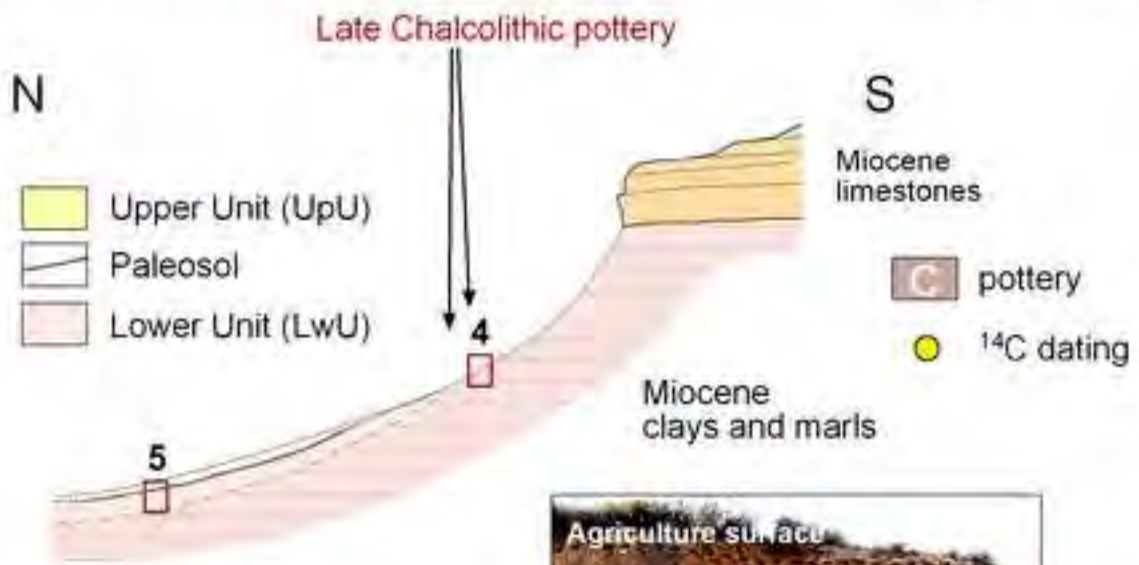


Figure 4

[Click here to download high resolution image](#)



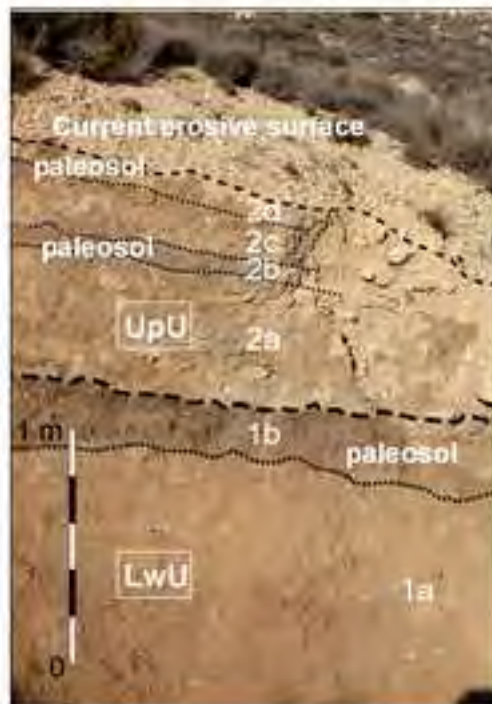
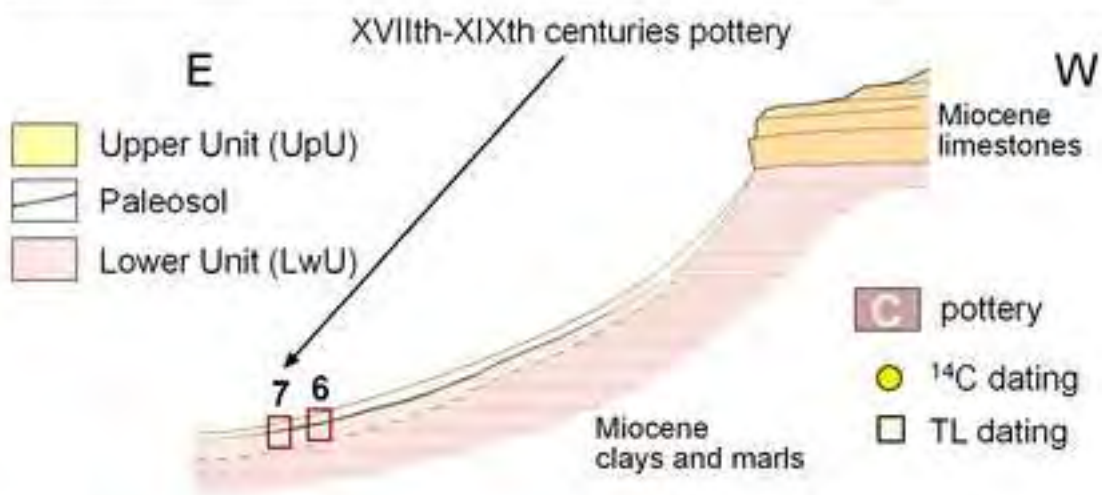
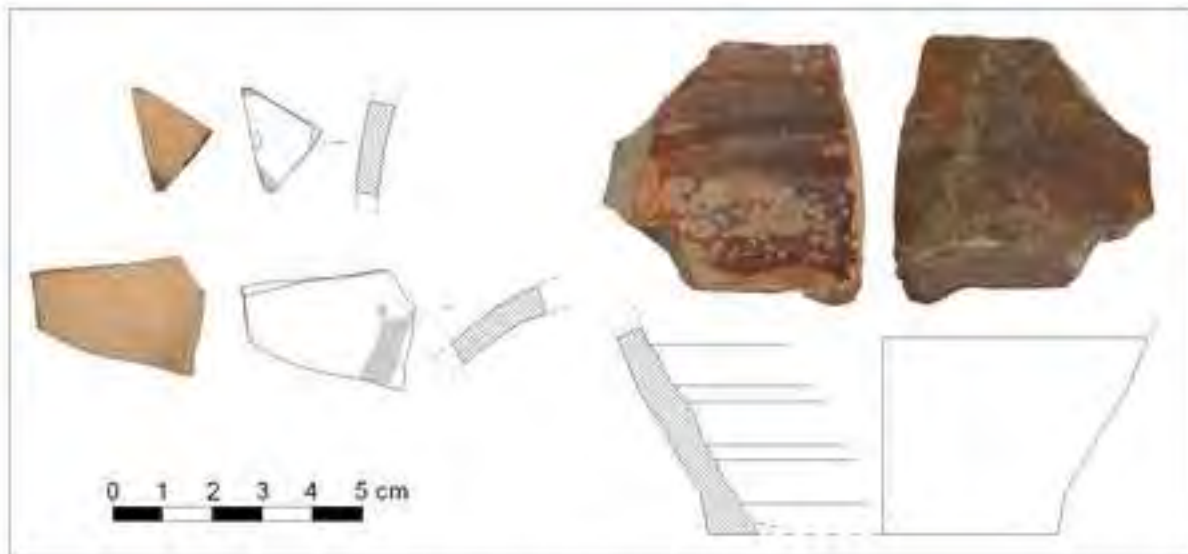
section 4



section 5

Figure 5

[Click here to download high resolution image](#)



section 6

section 7

Figure 6
[Click here to download high resolution image](#)

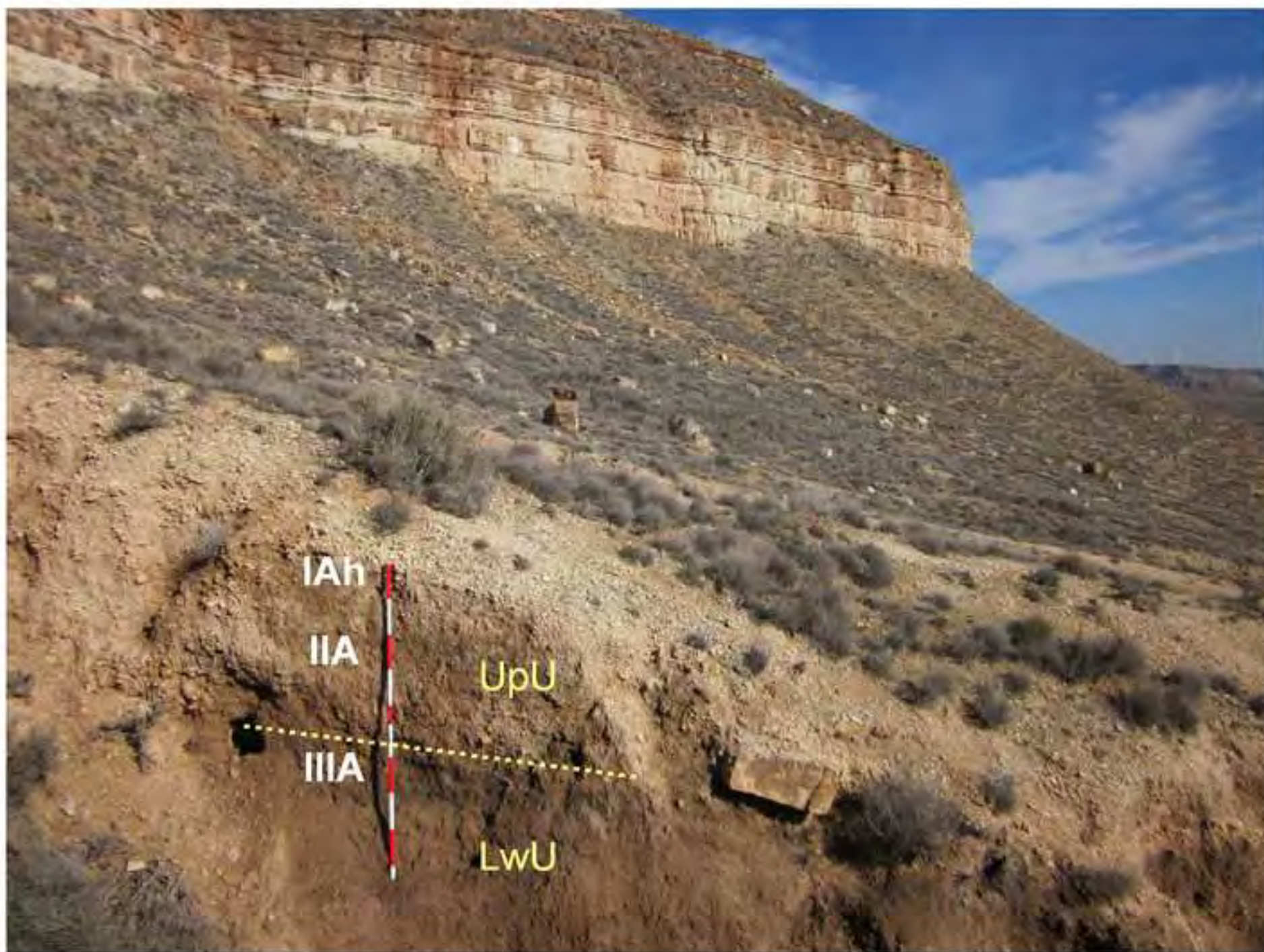


Figure 7
[Click here to download high resolution image](#)

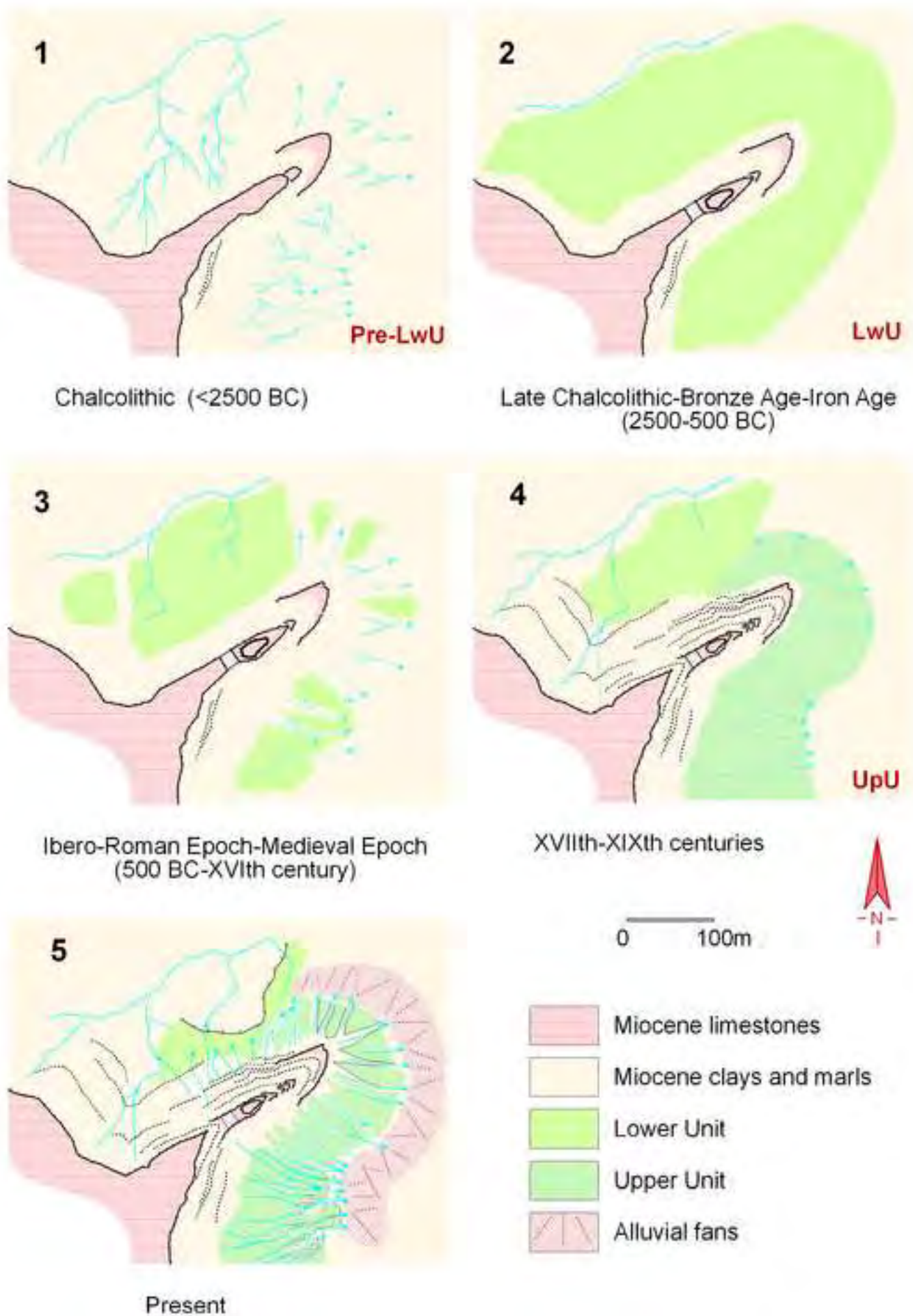


Figure 8

[Click here to download high resolution image](#)

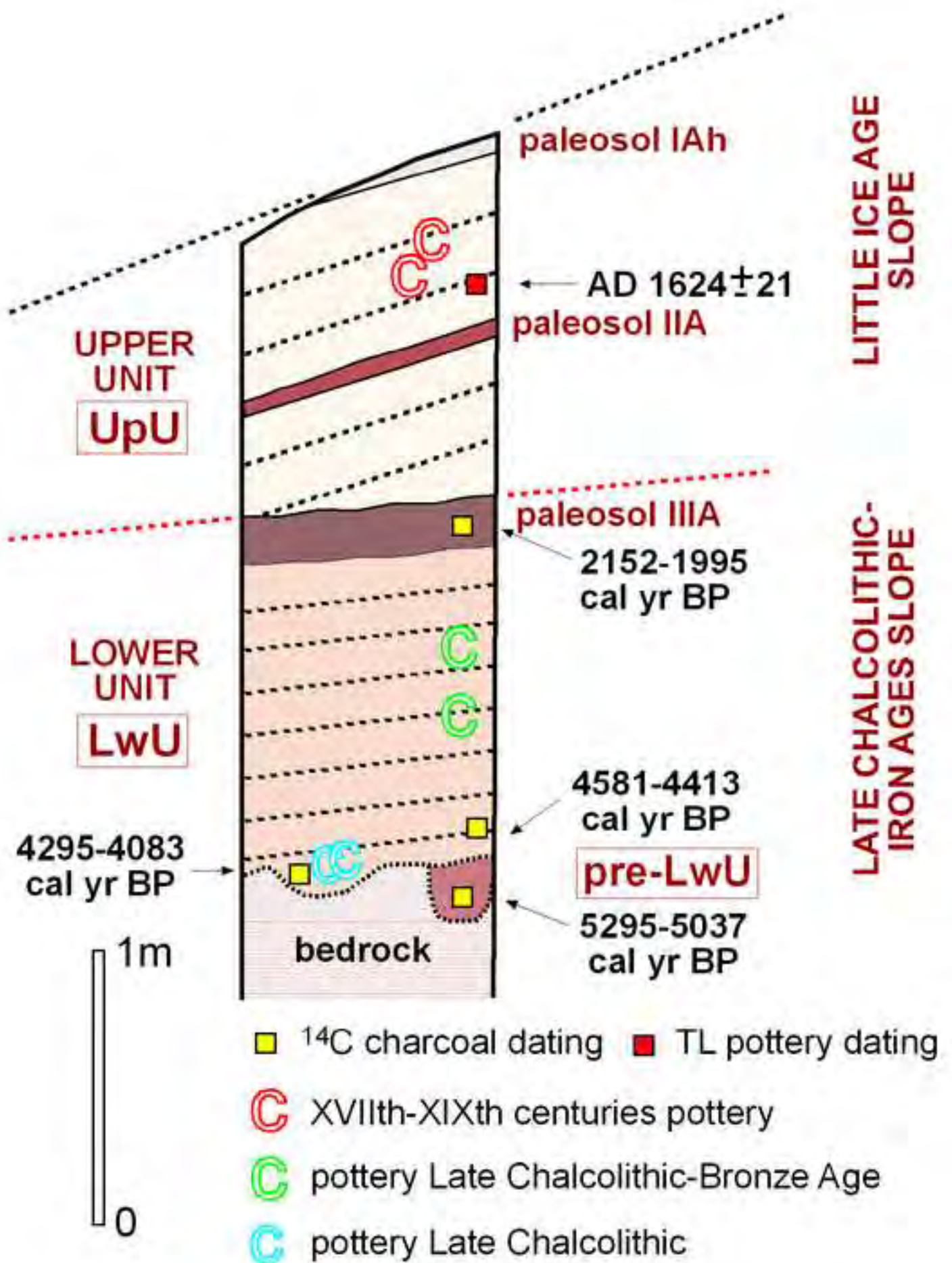


Figure 9
[Click here to download high resolution image](#)

